

**Contract No. and Disclaimer:**

**This manuscript has been authored by Savannah River Nuclear Solutions, LLC under Contract No. DE-AC09-08SR22470 with the U.S. Department of Energy. The United States Government retains and the publisher, by accepting this article for publication, acknowledges that the United States Government retains a non-exclusive, paid-up, irrevocable, worldwide license to publish or reproduce the published form of this work, or allow others to do so, for United States Government purposes.**

**FE-11-1369**  
**COMPARISON OF EXPERIMENTS TO**  
**CFD MODELS FOR MIXING USING**  
**DUAL OPPOSING JETS IN TANKS WITH**  
**AND WITHOUT INTERNAL**  
**OBSTRUCTIONS**

**Robert A. Leishear**

e-mail: Robert.Leishear@srnl.doe.gov  
Savannah River National Laboratory  
Aiken, S. C., 29803, USA

**Si Y. Lee**

e-mail: Si.Lee@srnl.doe.gov  
Savannah River National Laboratory  
Aiken, S. C., 29803, USA

**Mark D. Fowley**

Mark.Fowley@srnl.doe.gov  
Savannah River National Laboratory  
Aiken, S. C., 29803, USA

**Michael R. Poirier**

Michael.Poirier@srnl.doe.gov  
Savannah River National Laboratory  
Aiken, S. C., 29803, USA

**Timothy J. Steeper**

Timothy.Steeper@srnl.doe.gov  
Savannah River National Laboratory  
Aiken, S. C., 29803, USA

## **ABSTRACT**

*This paper documents testing methods, statistical data analysis, and a comparison of experimental results to CFD models for blending of fluids, which were blended using a single pump designed with dual opposing nozzles in an eight foot diameter tank. Overall, this research presents new findings in the field of mixing research. Specifically, blending processes were clearly shown to have random, chaotic effects, where possible causal factors such as turbulence, pump fluctuations, and eddies required future evaluation.*

*CFD models were shown to provide reasonable estimates for the average blending times, but large variations -- or scatter -- occurred for blending times during similar tests. Using this experimental blending time data, the chaotic nature of blending was demonstrated and the variability of blending times with respect to average blending times were shown to increase with system complexity. Prior to this research, the variation in blending times caused discrepancies between CFD models and experiments. This research addressed this discrepancy, and determined statistical correction factors that can be applied to CFD models, and thereby quantified techniques to permit the application of CFD models to complex systems, such as blending. These blending time correction factors for CFD models are comparable to safety factors used in structural design, and compensate variability that cannot be theoretically calculated.*

*To determine these correction factors, research was performed to investigate blending, using a pump with dual opposing jets which re-circulate fluids in the tank to promote blending when fluids are added to the tank. In all, eighty-five tests were performed both in a tank without internal obstructions and a tank with vertical obstructions similar to a tube bank in a heat exchanger. These obstructions provided scale models of vertical cooling coils below the liquid surface for a full scale, liquid radioactive waste storage tank. Also, different jet diameters and different horizontal orientations of the jets were investigated with respect to blending.*

*Two types of blending tests were performed. The first set of eighty-one tests blended small quantities of tracer fluids into solution. Data from these tests were statistically evaluated to determine blending times for the addition of tracer solution to tanks, and blending times were successfully compared to Computational Fluid Dynamics (CFD) models. The second set of four tests blended bulk quantities of solutions of different density and viscosity. For example, in one test a quarter tank of water was added to a three quarters of a tank of a more viscous salt solution. In this case, the blending process was noted to significantly change due to stratification of fluids, and blending times increased substantially. However,*

*CFD models for stratification and the variability of blending times for different density fluids was not pursued, and further research is recommended in the area of blending bulk quantities of fluids. All in all, testing showed that CFD models can be effectively applied if statistically validated through experimental testing, but in the absence of experimental validation CFD model scan be extremely misleading as a basis for design and operation decisions.*

## **INTRODUCTION AND RESEARCH SUMMARY**

The primary reasons for this research were to establish the minimum design requirements for a pump, the blending times required to operate that pump at full scale, and other design requirements not discussed at all in this paper. Specifically, this paper focuses on blending times and how to quantify them, using CFD models, experiments, and analysis to describe blending in a pilot scale tank. Although scale-up is not discussed here, a primary purpose of the research was to scale-up blending processes and equipment to 4.62 million liter (1.22 million gallon), 25.91 meter (85 foot) diameter, radioactive liquid waste storage tanks at Savannah River Site (SRS) in Aiken, South Carolina. A series of Conference papers summarize the full extent of this research (Leishear, et al. [1-4]), and Savannah River National Laboratory (SRNL) reports provide comprehensive experimental data and analysis from the research (Leishear, Lee, et al. [5-8]). In short, this paper compares blending times calculated from Computational Fluid Dynamics (CFD) models to experimental results for pilot scale testing in a geometrically scaled, 2.44 meter (8 foot) diameter tank with sub-surface obstructions representing cooling coils, which were both installed and removed from the pilot scale tank during testing. The reader is referred to [1-6] for scale-up methods for blending times and other aspects of this blending research, which are specifically related to radioactive liquid

waste processing. Developed from [1-6], this paper focuses on the blending of two fluids, which is applicable to the more general field of industrial mixing theory.

Comprehensive descriptions of testing and analysis techniques are provided here to clearly explain and prove assumptions, results, and conclusions. Some of the equipment descriptions and analyses could be deleted from this text without a significant loss in continuity of the analysis, but these descriptions provide a comprehensive explanation of the experimental techniques and justifications for the conclusions with respect to blending times.

In general, the average blending times were adequately predicted, but the variability in blending times increased dramatically as the system complexity increased. In fact, failure to recognize this variability may lead to serious errors in system design and the prediction of blending times. Overall, increasing the complexity of a process increases the variability of a measured variable for that process. In this case, the blending times increase with system complexity.

This increase in complexity is consistent with conclusions from chaos theory. Although chaos theory (Bai-Lin [9]) is not discussed in this paper, a general conclusion from chaos theory is that stochastic analyses, rather than deterministic equations are required to describe system processes as they become more complex. For this work, deterministic equations are expressed in terms of CFD models, which are derived from the fundamental equations of motion throughout fluids in a tank using the CFD program Fluent<sup>®</sup>. Once the deterministic models for blending times were obtained using Fluent<sup>®</sup>, statistical analyses were applied to those times by assuming that the standard Gaussian probability distribution describes the range of applicable solutions.

In particular, CFD models of increasing complexity were compared to experimental results for examples where tracer quantities of one solution were blended with large quantities of another solution. The most simplistic model was a cylindrical tank with a single mixing jet pointed upward toward the surface. For this model, the statistical variance was 24 %. The next most complicated model employed dual opposing jets for blending in a cylindrical tank with a center column, which obstructed blending. For this model, the statistical variance of the blending time from the average was 74 percent. The most complicated model considered in this study involved a cylindrical tank with dual opposing nozzles, a central column, and hundreds of vertical obstructions used to model cooling coils in a larger scale tank. Similar to tubes in a heat exchanger, these obstructions resulted in a statistical variance from the average blending time equal to 164%.

From the data, correction factors, or safety factors, were applied to CFD results to adequately predict the expected blending times for different design conditions. For a single jet in a tank without obstructions, the correction factor equaled 1.24. For dual jet blending in a tank with a single obstruction in the center, the correction factor equaled 1.74. For dual jet blending in a tank with numerous obstructions, the correction factor equaled 2.64. To use the correction factors, the CFD predicted blending times are multiplied by the correction factor.

When the fundamental mixing processes were altered for this testing, the correction factors varied significantly. Specifically, four tests were performed in a tank with cooling coil models and dual opposing blending jets for a process referred to here as bulk addition blending, as opposed to blending of tracers. In these tests, one quarter of the

tank contents were removed from the tank, and were altered to be monitored when blended with the remaining fluid in the tank. When the two different fluids were blended, blending behavior was completely different than the blending observed during tracer additions to the tank. When a heavier fluid was added from the top of the tank into a lighter fluid, the action of simply adding the fluid to the tank was sufficient to fully blend the tank contents. Similarly, when two fluid of equal density were blended, fluid addition was adequate to blend the tank contents. However, when a lighter fluid was added to a heavier fluid from above the fluid surface, the blending time increased by a factor of ten for the performed test, suggesting that the correction factor equaled, ten or more. CFD models and statistical variance were not investigated for bulk fluid blending, and further research is recommended.

Although correction factors have not been typically applied to CFD blending models in the past, the use of correction factors, or safety factors, is long standing in mechanics. For example, a safety factor, or design margin of three with respect to the ultimate strength of a material is used for ASME, B31.3 Process Piping design. Another example of the use of safety factors is inherent in the use of fatigue data for the failure of materials in machine, piping, or pressure vessel designs. The number of cycles to cause fatigue cracking is commonly provided in the literature as an average number of cycles to failure at a specific applied stress, or strain, on a specimen. However, the experimental data is typically plus or minus an order of magnitude (plus or minus a factor of ten) for the number of cycles to failure. For fatigue failure analysis, the variation -- or scatter -- about the average number of cycles needs to be considered. Similarly, the scatter needs to be considered for complex fluid processes, such as average blending times.

In short, experiments and models yielded two interesting results. First, the variation in blending times for tracer additions to a tank increased markedly as the system complexity increased. Second, when the blending process was changed from tracer addition blending to bulk addition blending, the blending times drastically varied even more and were shown to be a function of the difference in density and viscosity between the two fluids. Heavier fluids added into lighter fluids reduced the blending time and lighter fluids added into heavier fluids increased the blending times. In the absence of pilot scale testing, CFD modeling alone would have been inadequate, but safety factors validated the use of CFD models for some complex blending processes, and other processes may be further investigated using the techniques presented here.

## **LITERATURE REVIEW AND COMPARISON TO CFD MODELS**

Although blending research is limited for blending in tanks with geometry similar to the tanks considered here, much research has been performed for blending in tanks using jets. Accordingly, a literature review is summarized here to describe the present level of understanding for blending time predictions, using a single jet. Also, some CFD modeling was performed during this research for comparison to the literature. This literature review showed that the single jet blending time can be modeled by an equation, which has a correction factor of about 24 %. A CFD model was also performed for the work cited here, and the CFD model was within 3% of the blending time predicted by equation. A discussion of the literature review and single jet CFD modeling follows.

### **Literature Results for Blending Time Equations**

Dimenna, et al. [10] provided a recent survey of blending research applicable to nuclear waste storage tanks, and Grenville and Tilton [11, 12] provided an excellent summary of blending research for experiments in open tanks up to 9.84 million liter (2.6 million gallon) capacity, which were mixed using a single nozzle jet positioned from a lower corner of the tank and aimed upward toward the fluid surface at the far side of the tank. Also, some work has been completed to compare CFD models to experimental results for single mixing jets (Patwardhan [13] and Rahimi and Parvareh [14]).

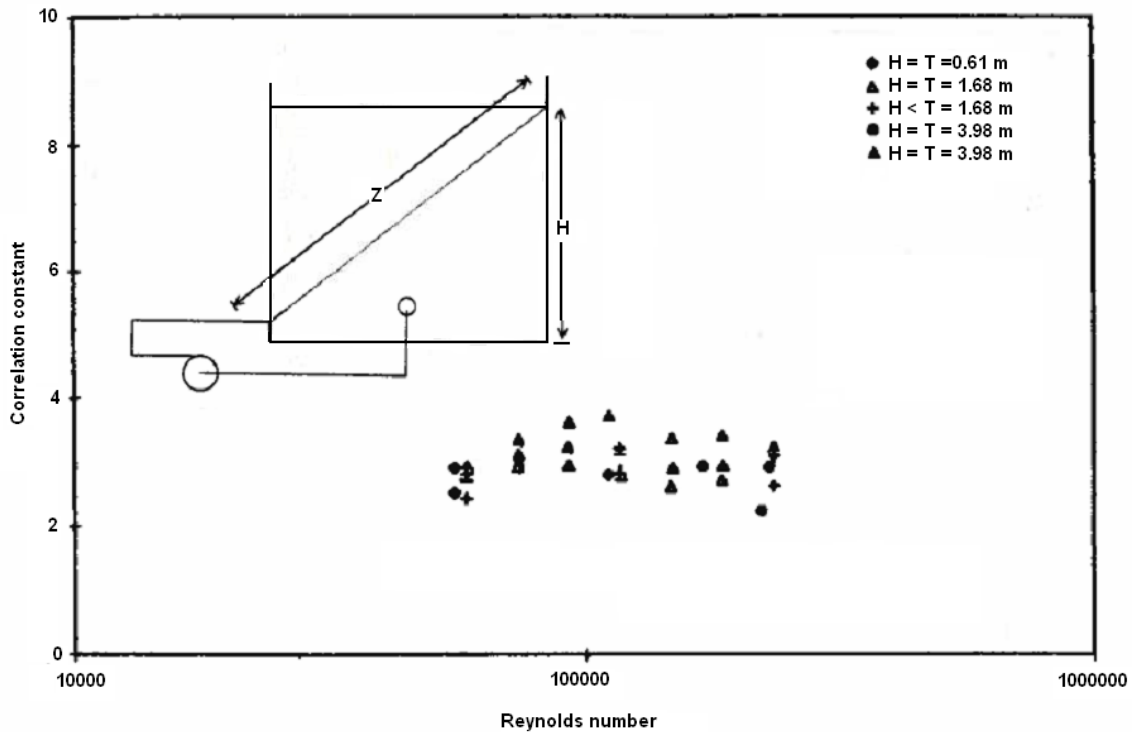


**Figure 1: Blending test results for a single nozzle (Grenville [11, 12])**

Grenville [11, 12] performed a number of experiments in addition to evaluating research from others, using the tank geometry shown in Fig. 1, where  $H$  is the height of the fluid, and  $Z$  is the path length of the jet. From these data, Grenville and Tilton expressed the blending time as

$$t = (C \cdot T^2) / (U_o \cdot D) = (3.00 \cdot T^2) / (U_o \cdot D) \quad (1)$$

where the blending time,  $t$ , was expressed in terms of the tank diameter,  $T$ , an experimentally derived correlation factor,  $C$ .  $U_o D$  is a pump design parameter, which is the product of the nozzle exit velocity,  $U_o$ , times the nozzle diameter,  $D$ . Grenville and Tilton's work also considered the effects of the jet angle to a horizontal plane, where the blending time increases as the jet angle decreases toward the floor of the tank.

Grenville and Tilton's data pertinent to this research are summarized in terms of Reynold's number at the nozzle exit in Fig. 1. Grenville and Tilton also noted that the standard deviation ( $\sigma$ ) for blending times for this data was 11.85%. The  $2\sigma$  variation (Coleman and Steele [15]) for a 95% confidence level was therefore approximately  $23.7\% \approx 24\%$ .

### **CFD Models for Blending Times Using a Single Jet**

CFD models were performed for a single jet design as shown in Figs. 2 and 3 to support the present research (Lee, et al. [8])). These results were consistent with Grenville's research. In fact, the CFD model listed in Table 1 was within 3% of the blending time predicted by Equation 1.

The simplified Equation 1 can express the blending time for tanks without obstructions and with a single jet installed, and, as discussed below, this equation may be adapted to a tank with dual opposing nozzles and a single central column for some nozzle flow rates. However, for the more general case of blending in a tank with many obstructions, Equation 1 is inadequate to describe the blending times in a tank.

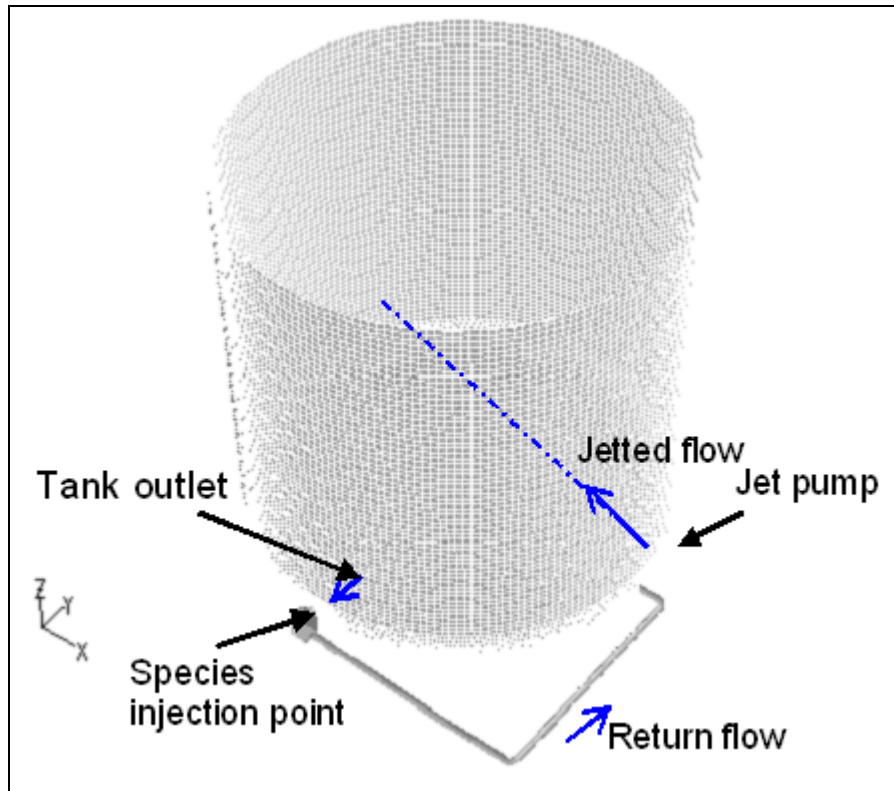


**Figure 2: Tank geometry for species transport calculations**

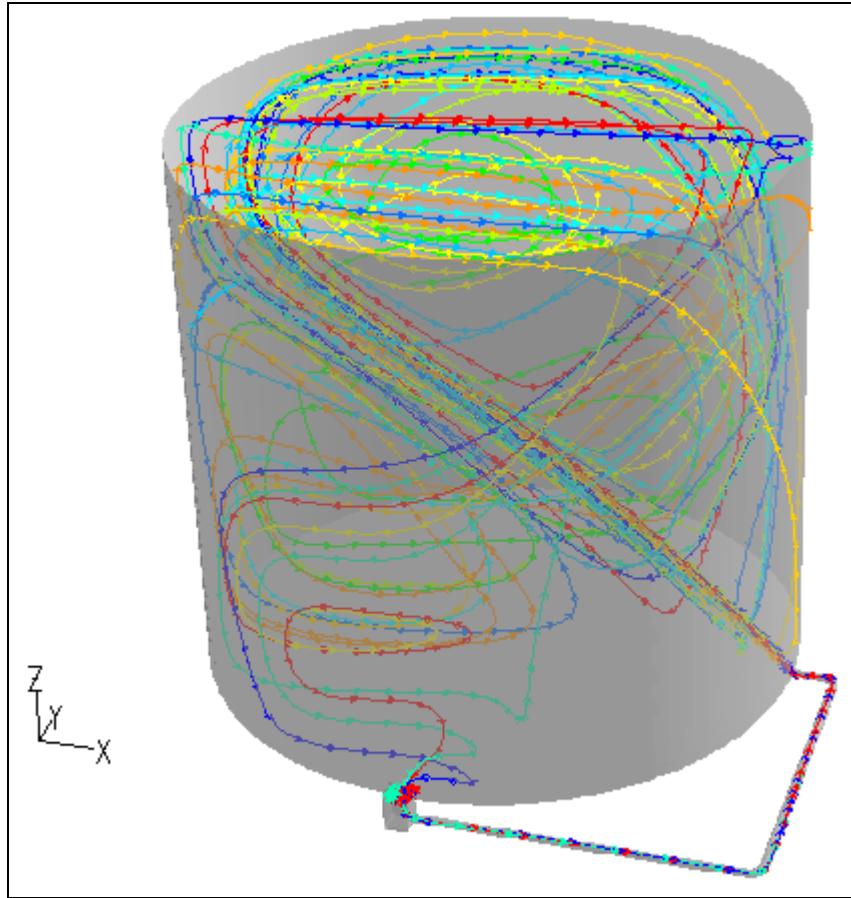


**Figure 3: CFD model for a single upward pointing jet used during tank blending**

**Table 1: Test conditions for transient CFD calculations**

	$T$ (Tank dia.)	$H$ (liquid height)	Inclination angle of Jet*	$D$ (jet dia.)	$U_o$ m/sec	Mixing time
Tank Dimensions	1.68 m	1.55 m	42.6°	26.1 mm	19.8	32 sec.

Note: Jet is located at the corner of tank bottom as shown in Figure 2.

**Literature Results for CFD Comparisons to Measured Blending Times**

Using standard  $\kappa$ - $\epsilon$  turbulence models and experimental data, Patwardhan [13] showed that CFD models may be used in lieu of Equation 1 to provide estimates for blending times, as shown in Fig. 4. His tests in a 0.5 meter (1.64 foot) diameter tank were

performed using a setup similar to that shown in Fig.1. The variance between CFD estimates and experiment were not fully investigated, but some variation between CFD models and experimental results are evident from Patwardhan's results, where CFD and experiment varied by about 30% for one of his examples. Also note that the linear relationship assumed in Equation 1, may not be applicable as flow patterns in the tank are complicated by nozzle position with respect to the tank bottom. The stochastic nature of blending begins to surface from Patwardhan's test results.

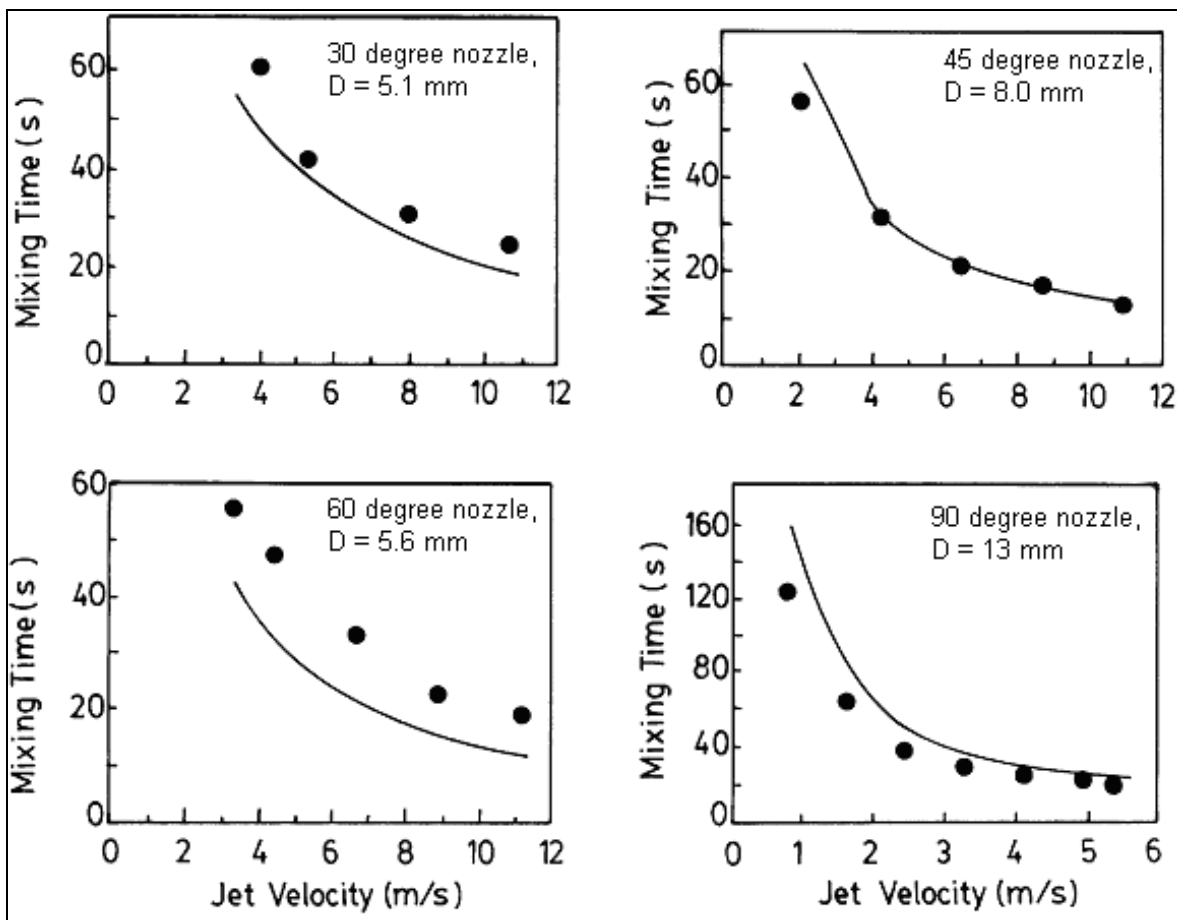


**Figure 4: Comparison of CFD results to experiment in a 0.5 meter (1.64 ft) diameter tank for blending using a single jet, angled with respect to the tank bottom (Patwardhan [13])**

## TESTING TECHNIQUES

To understand the full scope of this pilot scale research, a brief summary of the required testing is followed by descriptions of the pilot scale equipment, test methods, and test results. As noted, tests for this research were of two basic types:

1) Blending of tracer quantities of acid, base, or dye into solution in the pilot scale tank. Acid and base solutions were added in a similar fashion for each test, while dual opposing jets blended the tank contents at steady state flow conditions for different values of  $UoD$ . Diffusion tests were also performed using tracer quantities.

2) Blending due to bulk addition of one solution into another in the pilot scale tank. This secondary set of tests was performed using viscous salt solutions and water, where visual observations of blending were coupled with pH measurements to determine blending times when bulk additions were made to the pilot scale tank.

For all testing, a data acquisition system (DAS) recorded jet flow rates,  $UoD$ , pH, and tank temperature (typically 70° F) for on line processing and post processing of data. Proportional-integral control was used to maintain constant flow rates during testing. All in all, tests and supporting measurements were carefully performed for repeatability, and instrument uncertainties, or inaccuracies, were shown to be negligible with respect to measured variables, such as pH which was used to establish blending times.

### **Test Setup for Blending of Tracers in the Pilot Scale Tank Using Jet Nozzles**

A schematic of the overall pilot scale test setup for most (81 tests) of the blending tests is shown in Fig. 5. Similar amounts of tracer quantities of dyes, acids, or bases were added to the tank at the chemical addition locations (B5 and C1 risers, Fig. 9), where the

choice of riser had a negligible effect on blending times. Tracers were blended using a recirculation pump that discharged the tank fluid through dual opposing nozzles.

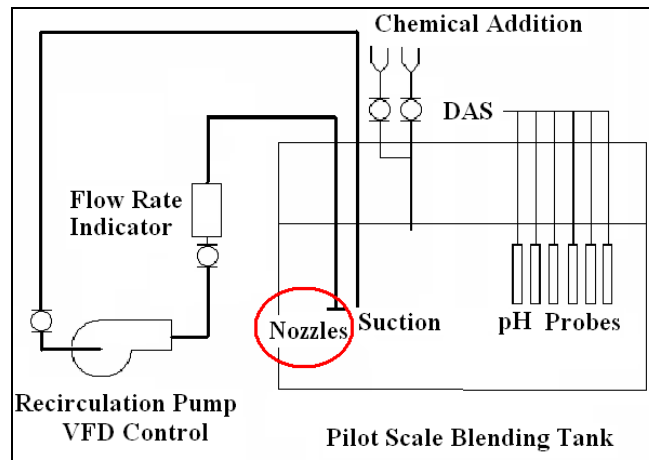


**Figure 5: Test schematic for acid, base, and dye additions**

### **Test Setup for Blending Due to Bulk Addition in the Pilot Scale Tank**

Tests for blending due to bulk addition (4 tests) used the same equipment except that pipe flow direction was modified, where an auxiliary storage tank supplied a salt solution or water to the pilot scale tank as required. Figure 6 shows the test schematic for bulk addition, where fluid discharged into the tank through a tube scaled down from a 3 inch schedule 40 pipe at 0.29 liters per minute (0.61 gpm, scaled down from 75 gpm). Once the bulk addition of fluid was completed to bring the tank up to the fill level, the blending pumps were operated by changing valve positions to obtain the operating schematic shown in Fig. 5. The pH was monitored throughout these processes to understand the effects of bulk addition on blending.

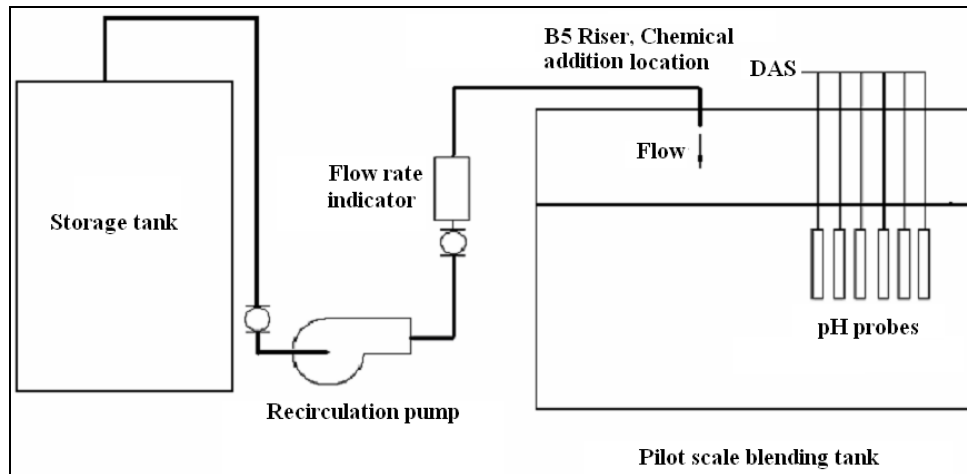


**Figure 6: Test Schematic for blending due to external bulk transfers into the pilot scale tank**

## **EQUIPMENT DESCRIPTION**

A pilot scale tank and components were modeled from a full scale tank at SRS, and instrumentation was added to perform pilot scale blending tests. Several different full scale tank designs are installed below grade at SRS. Some of the 51 SRS full scale tanks contain central roof support columns. Some tanks contain various cooling coil designs to remove residual heat from the radioactive decay of solids, which settle to the waste tank floors as a mixture referred to as sludge. Other design features irrelevant to pilot scale blending also vary between tanks, but are not discussed here. Only the pilot scale test results are reported here, and issues related to scale-up of those results are consequently neglected in this paper.

### **Pilot Scale Tank**

The pilot scale tank used during testing modeled one of the SRS tanks, which contained several miles of serpentine, 0.051 meter (2 inch), schedule 40, cooling coils on

typical 0.91 meter (36 inch) centers (Figs. 7, 8) and a central support column. All components below the planned operating liquid level at SRS were modeled at 1/10.85 scale. For test purposes, coil models were removable, and the support column was stationary (Figs. 7-11). To reference equipment locations, cylindrical openings through the full scale, concrete tank roof, referred to as risers, are visualized at pilot scale in Fig. 9. Acids and bases were added at the C1 riser location for Phase 1 tests, and were added at the B5 riser location for Phase 2 tests. Tests were performed in two phases, where test equipment was improved between phases. Primary modifications included a change in the location of the acid and base addition point (chemical addition point) from Riser C1 in Phase 1 to Riser B5 in Phase 2, and a change of the tank construction from opaque polyethylene to clear acrylic to improve test observations. The initial Phase 1 and final Phase 2 pilot scale, test setups are shown in Figs. 12 and 13 respectively, and these pilot scale models were modified slightly as required to perform different tests.

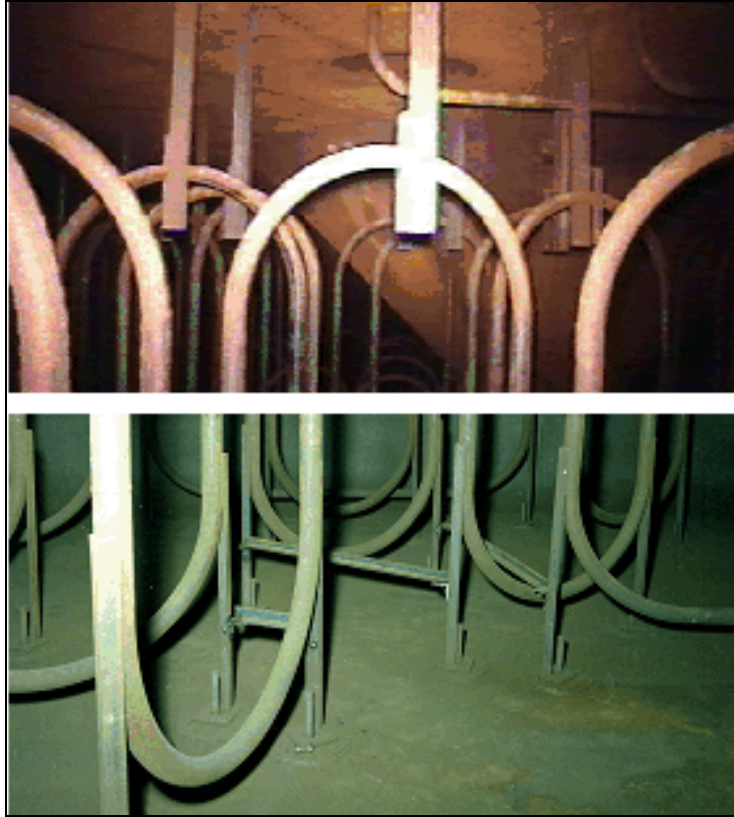


**Figure 7: Tank cooling coil design**

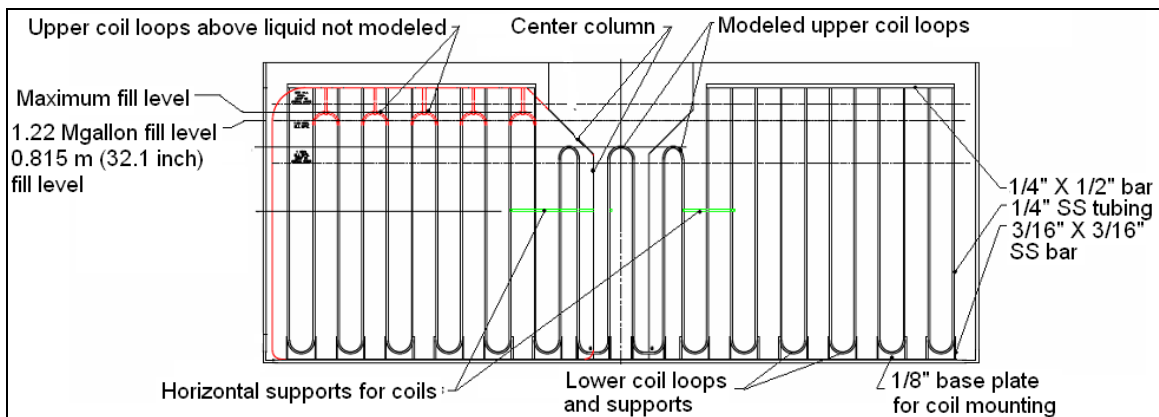


**Figure 8: Pilot scale blending tank model scaled from full scale tank, Elevation**





**Figure 10: Modeled cooling coils and center column assembly  
with overhead stiffeners and lifting lugs**

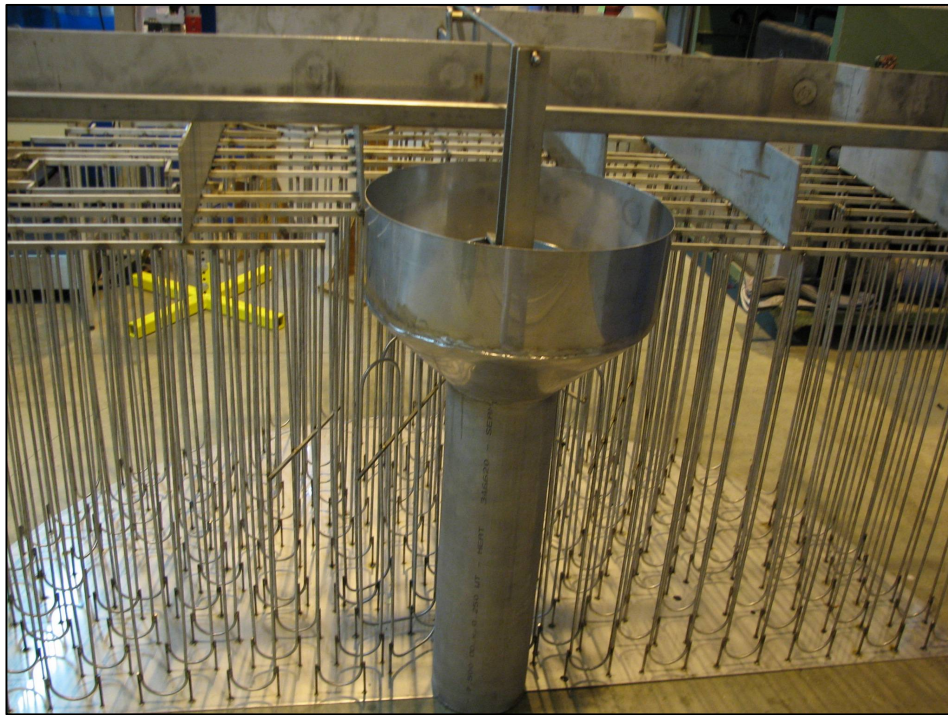


**Figure 11: Cooling coil assembly and center column**

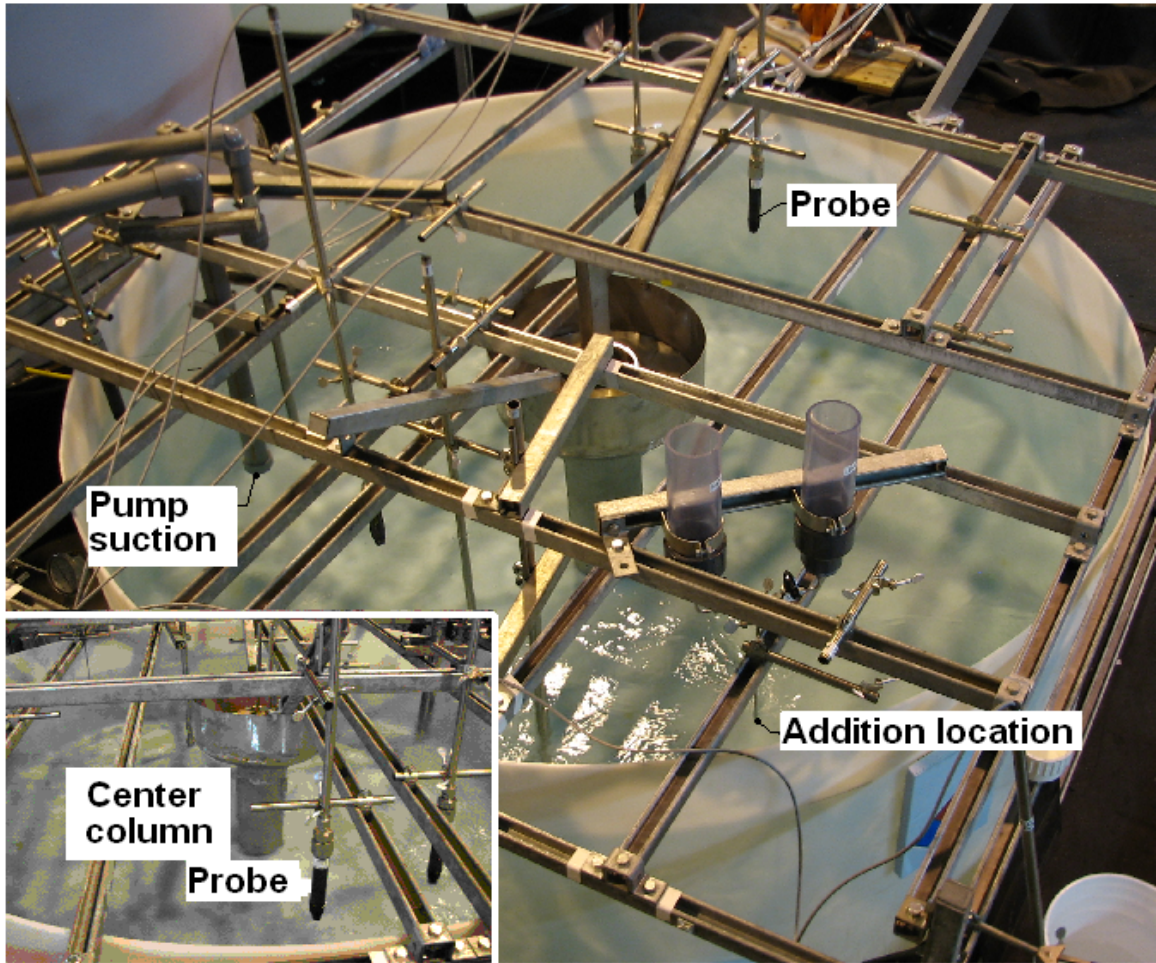


Figure 12: Phase 1, pilot scale tank, without cooling coil models

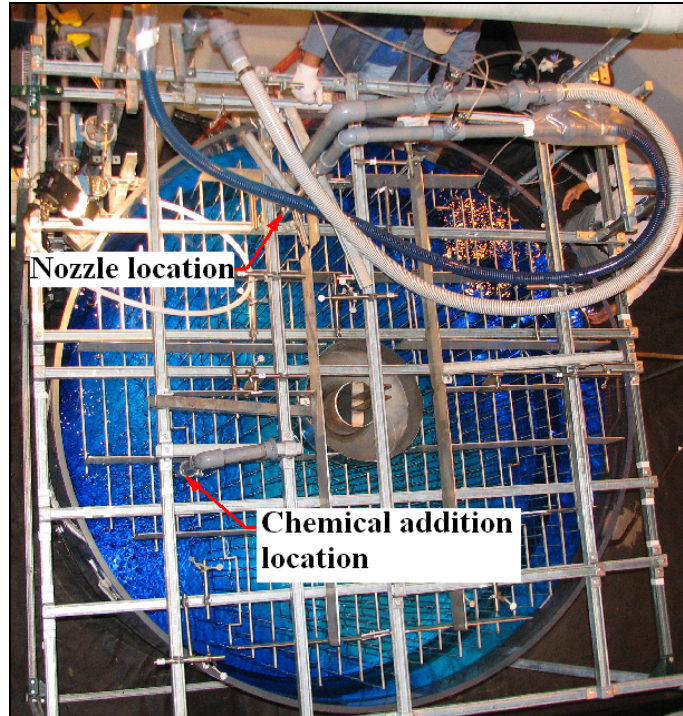


Figure 13: Phase 2, Pilot scale tank with cooling coil models installed

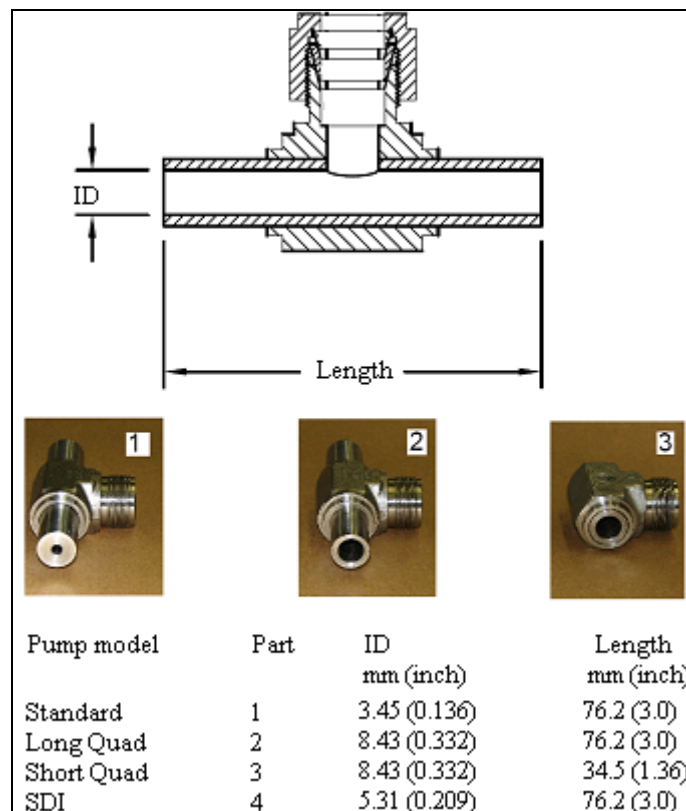
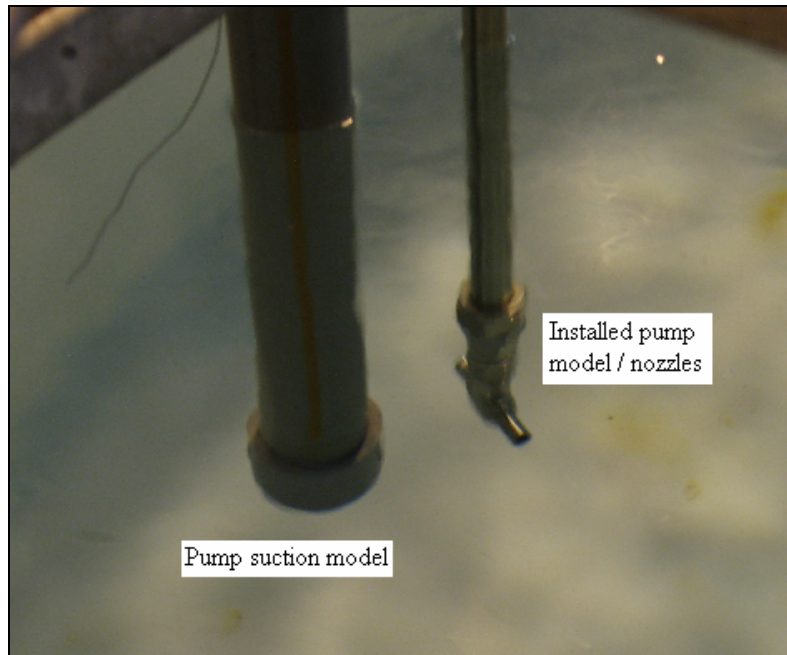


Figure 14: Initial pilot scale tee nozzle designs

## Pump Models

Pumps for blending were modeled as nozzles to investigate  $UoD$  and nozzle position effects on blending times. A variable frequency drive on the pump motor permitted variation of  $Uo$  at the nozzles, different nozzle designs varied  $D$  and the nozzle length, and the piping design permitted axial rotation of the nozzles with respect to the tank wall. The pump models were located at the mid-elevation of the fluid fill level for all testing, which was 0.408 meters (16.05 inches) from the tank bottom. Although different pump models were used as research progressed, modeled pump jet nozzles were consistently located at the B3 riser location (Figs. 9, 13).

Various models were investigated to determine their effect on blending performance, and assist the parallel design of a centrifugal pump required for blending by SRS [1]. The four initial pilot scale pump models consisted of horizontal nozzles (Figs. 14 and 15), which were fabricated from tubing tees. The names assigned to the different nozzle designs were associated with different full scale pump designs specific to SRS (SDI, Quad, or Standard [5, 6]), where diameters were 1/10.85 of full scale. A common suction pipe was used for tee pump models (Fig. 15), where the suction pipe cap had a hole drilled in the bottom to a prescribed dimension, which depended on the SRS pump model.



**Figure 16: Initial tee nozzle, design installation**

The final pump model design consisted of dual nozzles pointed 15 degrees upward to prevent sludge disturbance on the tank bottom, which was a separate requirement of this research [3, 6]. The final pilot scale design is shown in Figs 18 and 19, and is referred to as the CW pump design (Curtiss Wright, Inc.),  $D = 5.31$  mm (0.209 inch) diameter. A suction inlet was approximated from the full scale CW pump (Fig. 17), where details of the CW pump are available [6].

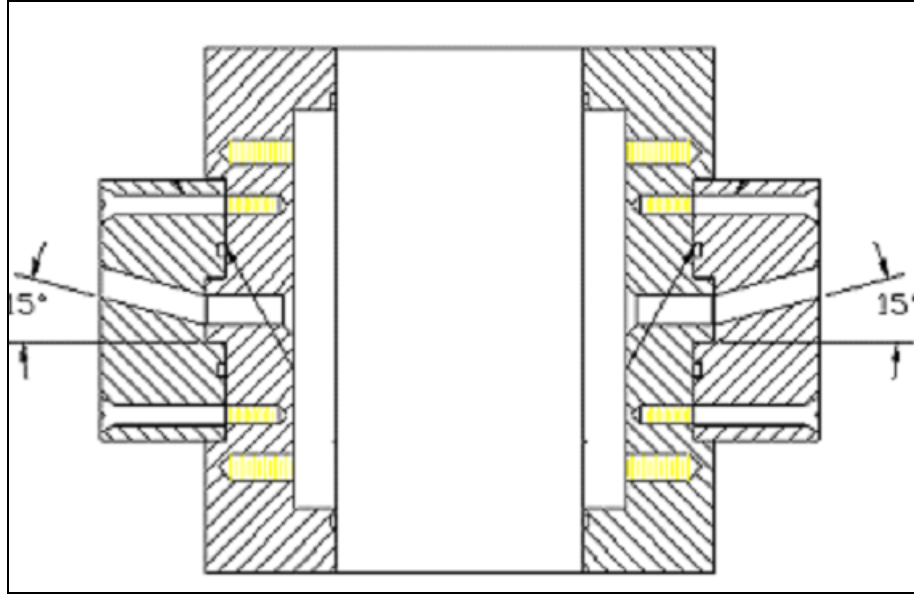


**Figure 16: CW pump model, cross section**

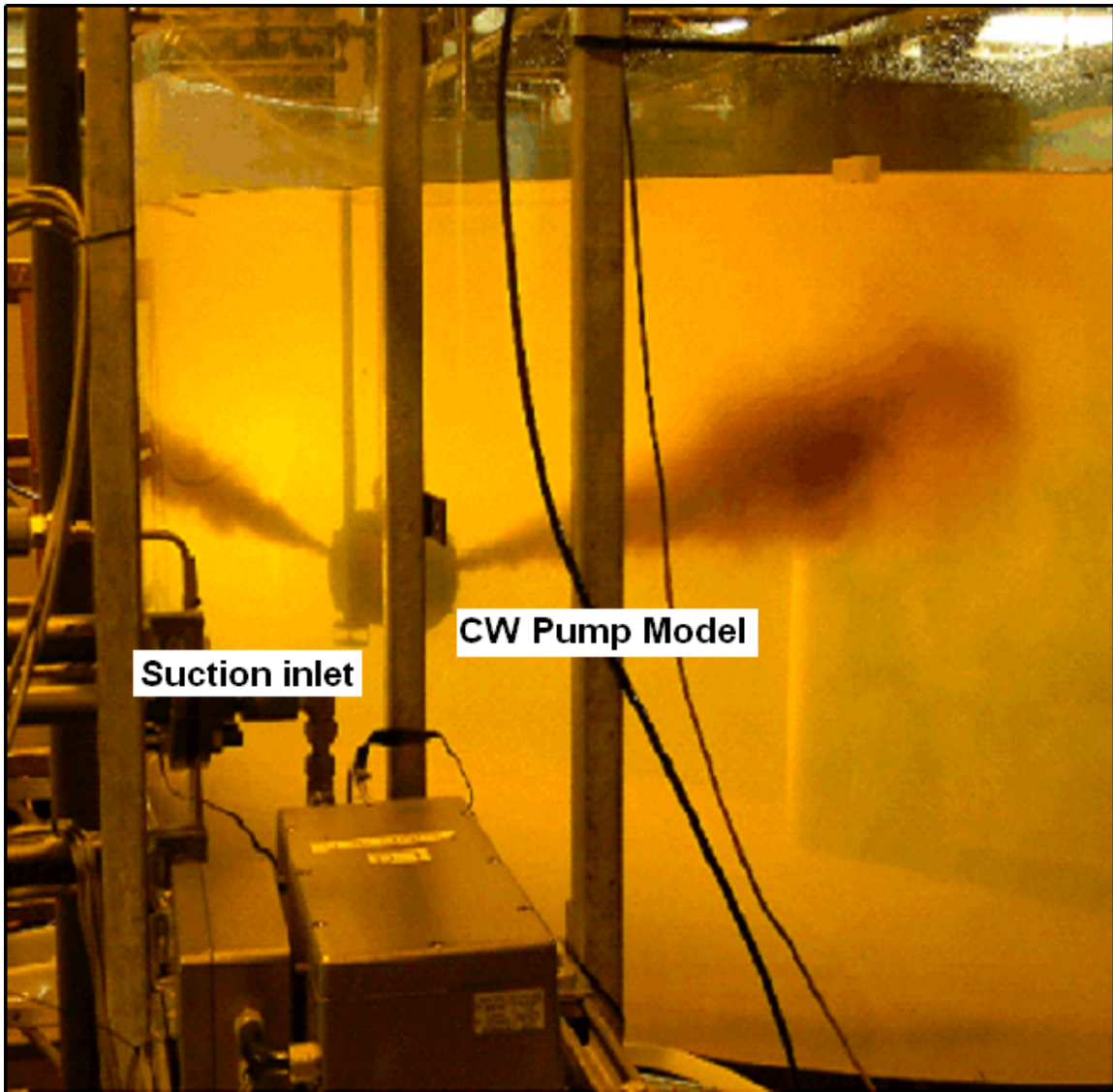


**Figure 17: Final CW pump model, operating in the pilot scale tank**

### **pH Probes**

Of the methods available to measure blending times (Paul, et al. [16]), pH monitoring was the primary technique selected for this research to obtain reasonable accuracy. As commonly practiced prior to this research, dye tests were performed to locate the positions where blending appeared to last occur in the tank. Probes 2, 4, 5, and 6 (Hach, Inc., pH probe model DPC1R1A) were located at these positions below the

surface, near the fill level. Probe 1 was located near the tank bottom, and probe 3 was located axially in line with one of the jet nozzles at the mid-height of the liquid. The probe locations are shown in Fig. 9. This research showed that the probe locations had little effect on determining blending times.

### Fluids Used for Testing

Newtonian fluids used for this research consisted of sodium nitrate salt solutions ( $\text{NaNO}_3$ ), water, sodium hydroxide ( $\text{NaOH}$ ), and nitric acid ( $\text{HNO}_3$ ). Measured viscosities and densities of the acids, bases, and salt solutions are listed in Table 2. For acid and base blending tests, 100 - 300 ml quantities of acid and base were added to the tank to obtain a range of 0.001 ( $4 < \text{pH} < 10$ ) throughout the tank. The total volume of water or salt test solutions in the pilot scale tank was 3758 liters (993 gallons).

**Table 2: Fluid Properties**

Fluid	Density gram/ml	Kinematic Viscosity Centipoise
Water	1.00	1.00
$\text{NaNO}_3$ + water for bulk transfers	1.32	2.26
Base additions, $\text{NaOH}$	1.16	2.68
Acid additions, $\text{HNO}_3$	1.14	1.07

## EXPERIMENTAL METHODS AND INSTRUMENTATION

Having described the test equipment, experimental methods and instrumentation warrant some discussion. Dye tests were initially performed to aid visualization of blending processes, and pH measurements were performed to quantify blending times during acid and base addition tests. To ensure that pH measurement techniques did not interfere with blending time calculations, instrument uncertainties were analyzed, and

other influences that could affect blending times, such as diffusion and buffering, were carefully evaluated and discounted as significant contributors to blending time calculations. Test numbers are referenced throughout this discussion, and may be gleaned from Appendix A: Tables 3 and 4, which are provided below.

### **Dye Tests**

The initial blending of acids or bases added to the tank were visualized by the use of a dye addition through the hopper (chemical addition location) above the tank. For one of the tests, shown in Figure 18, the dye flowed down to the tank floor, and then across the tank floor toward the pump suction. For higher flow rates, the tracer flowed across the upper fluid surface.

Blending time may also be affected if the location of the chemical addition point is close to the suction. For example, in one test (Test 39), dye was added directly to the pump suction piping, and the dye visually blended throughout the tank in about 30 seconds, which was much faster than other tests with comparable  $U_0D$ . Although dyes provide insight into the initial blending process, the continuing blending process required monitoring by another method.

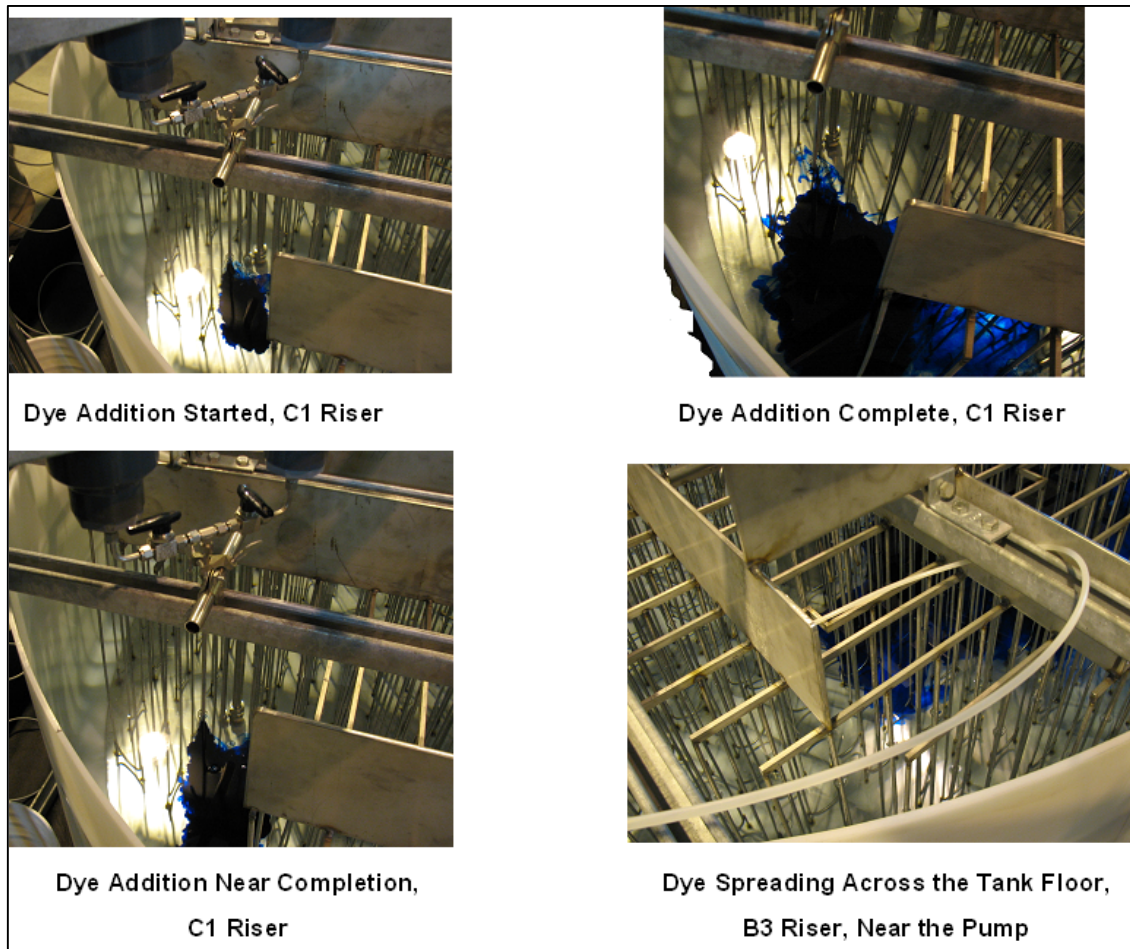


**Figure 18: Dye addition at C1 riser (Test 1)**

**Blending Performance and Blending Times**

To quantify blending performance, blending times were determined using commercial 95% blending criteria. The Hydronium ion concentrations  $[H_3O^+]$  were calculated from *pH* measurements and normalized to establish blending times for 95% mixing (Paul, et al. [16]). The 95% blending criteria is a commonly accepted criterion which defines the time following the addition of a tracer at which the concentrations throughout the tank are within  $\pm 5\%$  of the bulk concentration. Normalization is also a common practice for empirically quantifying mixing using concentration measurements.

From Paul, et. al. [16], *pH* probes are used to establish 95% blending times, which are determined from concentrations after adding a reactive tracer. To do so, a normalized concentration is calculated, where

$$C'_i = \frac{C_i - C_0}{C_\infty - C_0} \quad (2)$$

where  $C'_i$  equals the normalized concentration,  $C_i$  equals the measured variable concentration,  $C_0$  equals the initial concentration, and  $C_\infty$  equals the final equilibrium concentration. The 95% blending time equals the time required for the normalized probe output to reach and remain within 95 to 105%. Equation 2 is rewritten as

$$\text{Normalized } [H^+] = \frac{[H^+]_i - [H^+]_0}{[H^+]_\infty - [H^+]_0} \quad (3)$$

Some of the earlier Phase 1 tests were terminated prematurely, and Equation 4 was used from the literature (Paul et al. [16]) to predict the estimated blending time if the test had been run to completion.

$$t = t_n \cdot \frac{\ln\left(1 - \frac{95}{100}\right)}{\ln\left(1 - \frac{n}{100}\right)} \quad (4)$$

where  $t$  is the 95 % blending time,  $n$  is the percent blended, and  $t_n$  is a measured experimental blending time at known percent of blending. When required,  $t_n$  is determined at the time that testing was stopped. This approximation assumes that the normalized concentration converges to the value of 1 in a smooth logarithmic fashion.

Blending times obtained from this equation provide a reasonable approximation of the blending times for the tests under consideration.

### **Acid and Base Testing Using pH Measurements**

Test 11 is provided as an example of the use of test data combined with Equation 3 to establish a blending time. The raw data was displayed on the DAS in the format shown in Figure 19 during testing. The zero time,  $t = 0$ , equaled the time at which the valve on the hopper at the C1 riser location (Figs. 9, 12, and 18) was opened to release acid into the tank. The pump was already operating at the selected speed and flow rate.

Several steps were taken to calculate blending times. First,  $pH$  data was converted to hydronium ion concentrations as shown in Figs. 20 and 27. Then, the data was normalized to establish pilot scale blending times using Equation 2, as shown in Fig. 21. The accuracy of this technique bears some consideration.

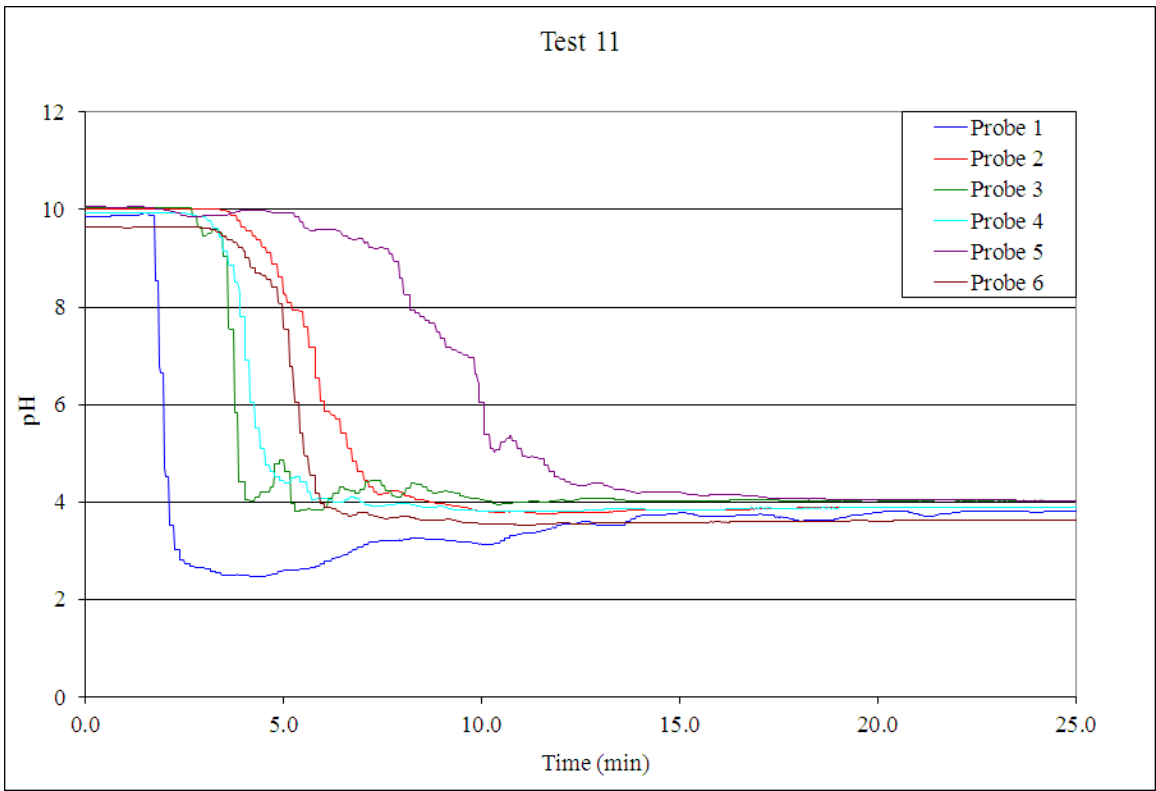
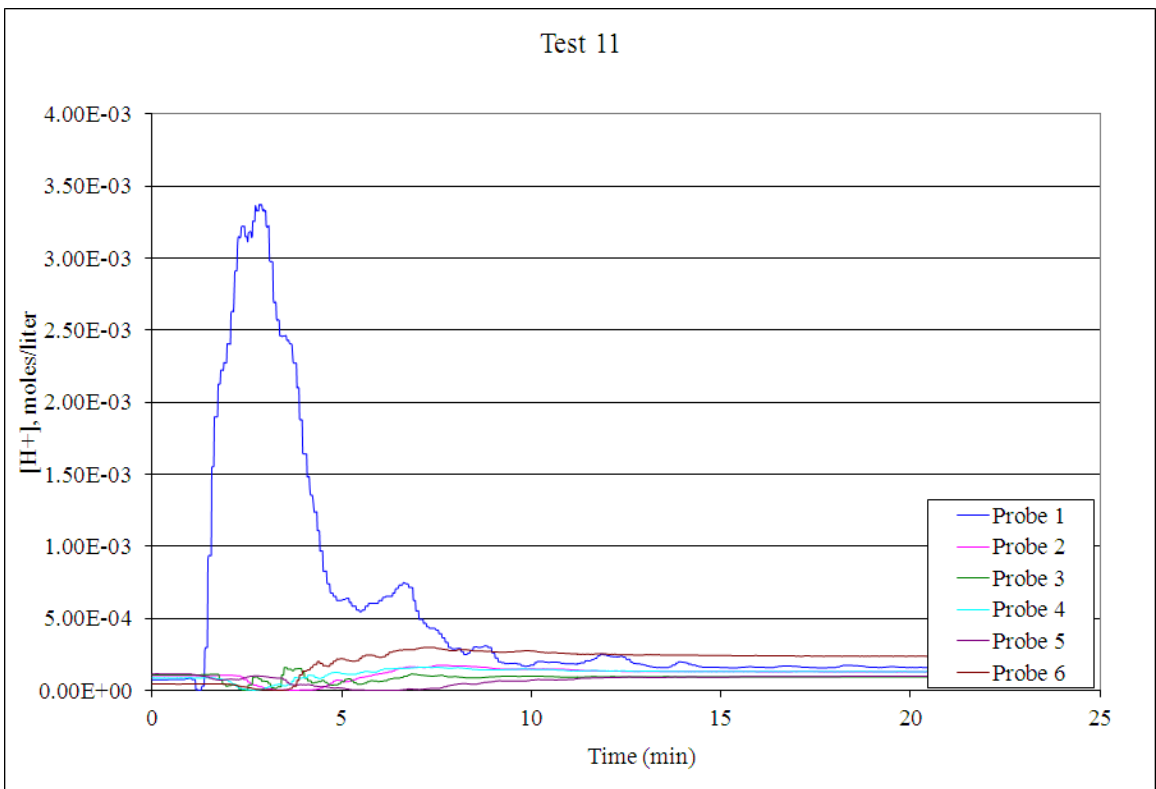
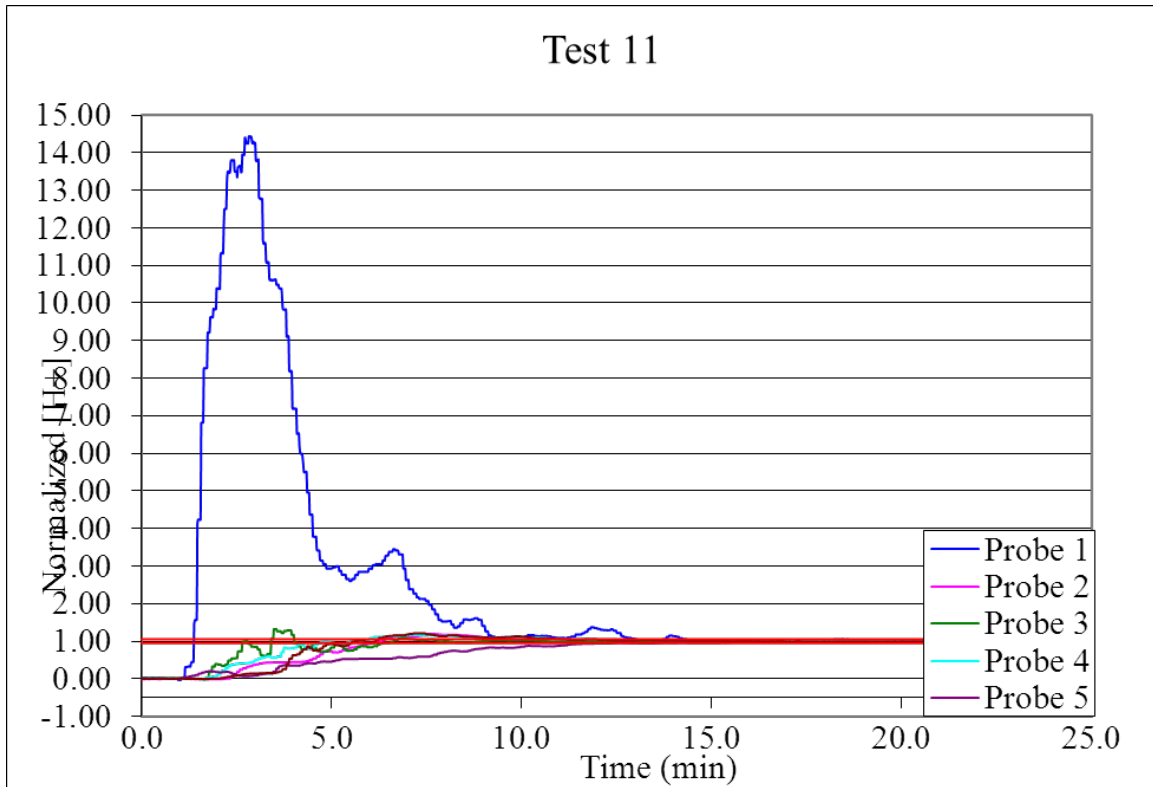


Figure 19: Raw pH data for analysis



**Figure 20: Concentration data for analysis**



**Figure 21: Normalized concentration data for analysis**

### **pH Uncertainty and Blending Time Accuracy**

Blending time accuracy is related to pH measurement uncertainty. However, blending times were negligibly affected by measurement uncertainties due to:

- 1) Small instrument errors,
- 2) Insignificant diffusion, and
- 3) Inconsequential buffering.

### *pH Probe Instrument Errors*

Instrument errors were negligible, and when combined with concentration variations, were shown to be as low as +/- 0.5% of the normalized concentration near equilibrium. To support this conclusion, statistical analyses were performed for test results with respect to instrumentation and blending time test data, where *pH* probes were located as shown in Fig. 9. Specifically, data sets similar to Fig. 22 had significant variability as the blending process proceeded, but the variability significantly reduced as the tank contents approached equilibrium. That is, the normalization technique provided a valid estimate of blending effectiveness near 95% blending. Also observed in the figure, some data scatter continues to exceed the initial 99% blending criteria, which indicated that 99% blending may not be accurately measured using *pH* probes. That is a 99% blending time is only approximate when used in a typical application for blending high quality products, such as pharmaceuticals.

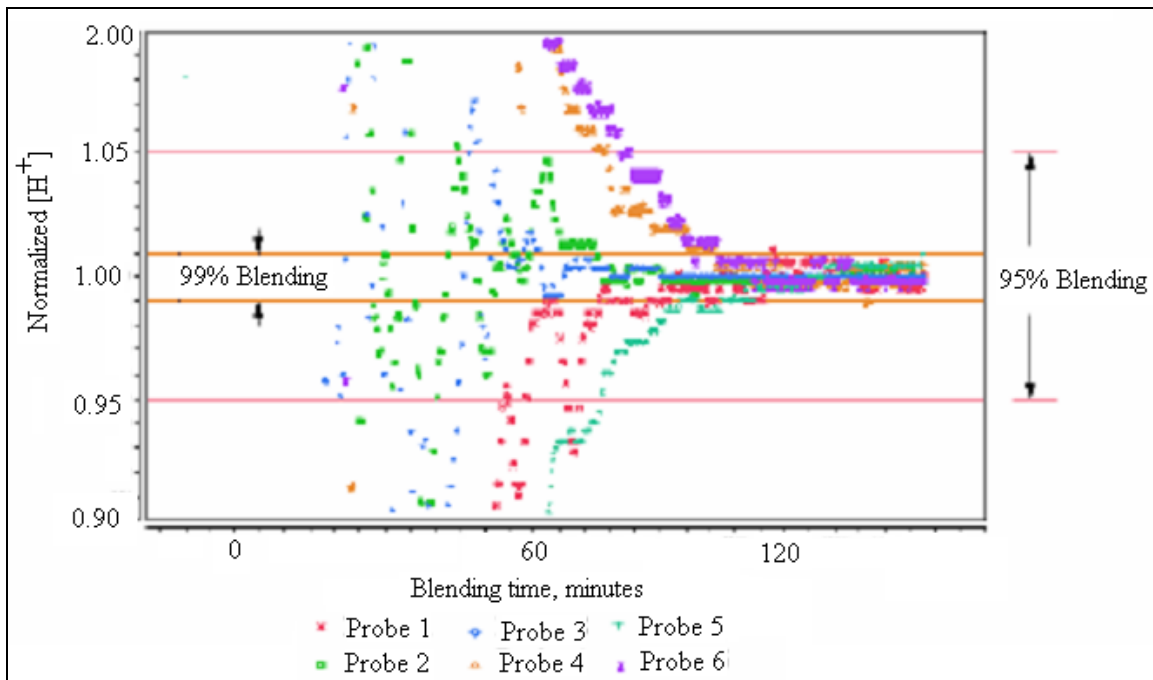


**Figure 22: Comparison of 95% blending to 99% blending (Test 21), T. Edwards**

### Buffering Effects on pH Measurements

Buffering of the solution was shown to affect pH values, but had a negligible effect on blending time predictions. Carbon dioxide in solution contributed a buffering effect to chemical reactions as carbonates and bicarbonates were formed. The concentrations of each chemical were not determined. However, the hydronium ion ( $\text{H}_3\text{O}^+$ ) was the measured blending parameter, and chemical reactions in solution therefore did not affect blending times. In other words, when the reactions were complete, hydronium ions were evenly distributed, and blending was complete. A comparison between measured Sodium concentrations and normalized  $[\text{H}^+]$  shows this anomaly in Fig. 23.

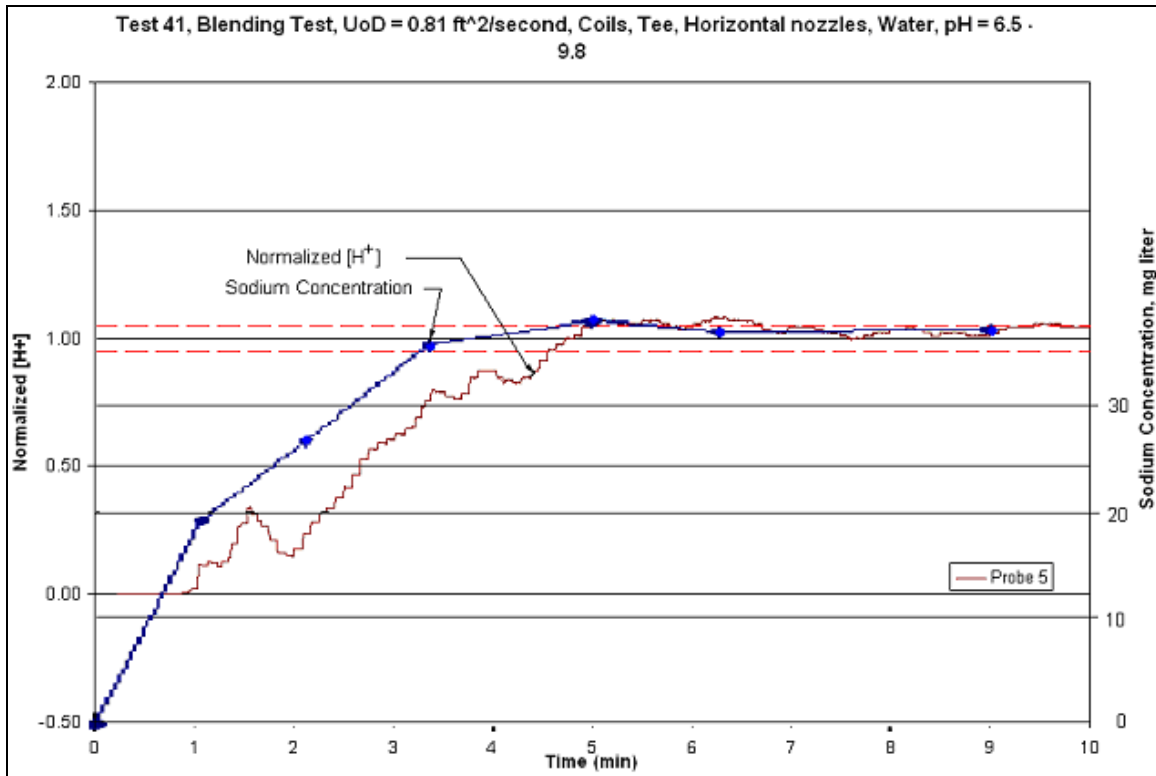


**Figure 23: Comparison of normalized hydrogen ion concentrations to measured sodium concentrations**

*Diffusion Effects on Blending*

Molecular diffusion was slow and had a negligible effect on blending, where diffusion was evaluated using dye, acid, and base tracers added to a still tank without mechanical agitation. A dye test was first performed to observe the diffusion process, and the blue dye was observed to rise in a laminar flow along the tank walls, and then circulate toward the center of the tank. Tests were also performed to evaluate diffusion by adding acid or base to the hopper, and measuring changes in pH (Figs. 24 and 25). The tank did not blend in more than 13-1/2 hours, which was considerably longer than any of the tests performed in Tables 3 and 4.

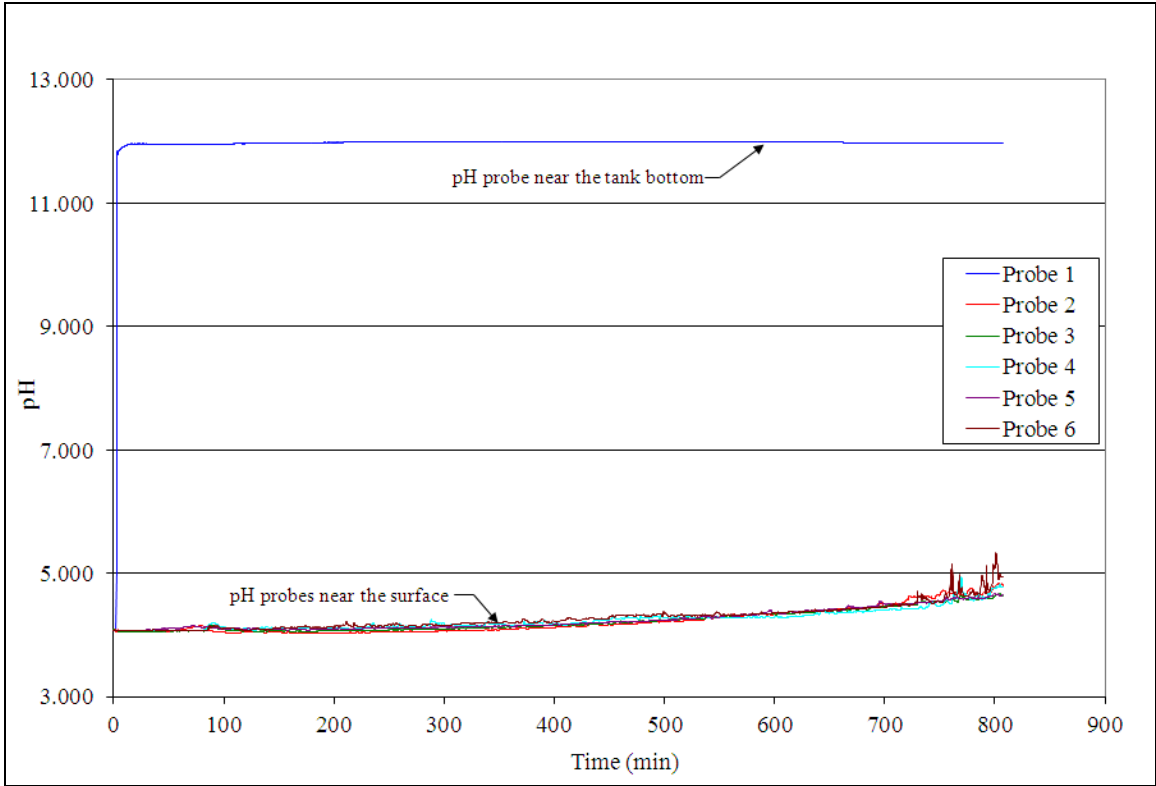


**Figure 24: Diffusion following a base addition, coils installed (Test 6)**

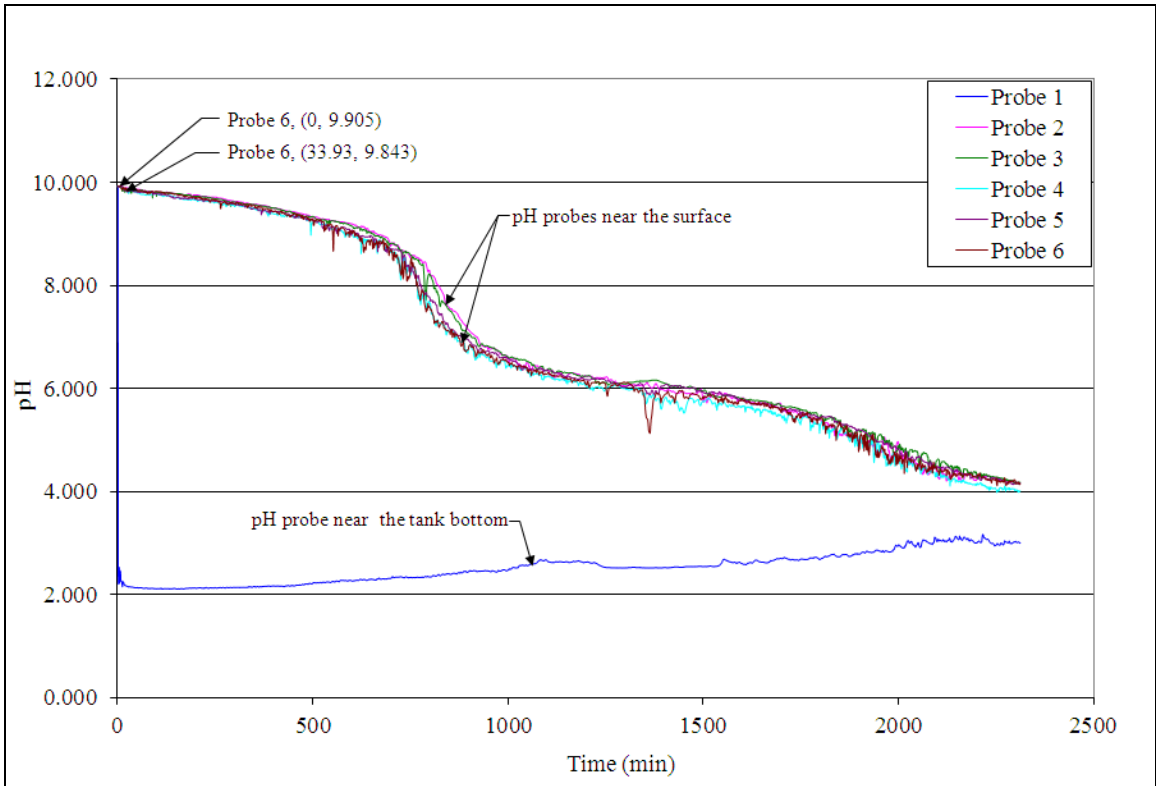


**Figure 25: Diffusion following an acid addition, coils installed (Test 7)**

## **TEST RESULTS FOR BLENDING OF TRACER SOLUTIONS**

Having validated an experimental method to measure blending times that method was used to find all test results listed in Appendix A: Tables 3 and 4. Phase 1 testing investigated horizontal nozzles and the effects of the nozzle orientation, or rotational position, with respect to the tank wall and changes in  $UoD$ . Phase 2 testing completed investigations for horizontal nozzle designs, but focused on the final, 15°, upward pointing CW nozzle design. Groups of similar tests for the CW nozzles were performed in Phase 2 to ensure repeatability of test results, and collect sufficient data for statistical analysis.

### **PHASE 1 BLENDING RESULTS FOR TRACER SOLUTIONS**

Phase 1 test results are displayed in Fig. 26 (Table 3, Appendix A). Numerous test details, and plots for all tests are available (Leishear, et al. [5, 6]). Blending times for Phase 1 tests are reported as the maximum blending time obtained from probes 1 - 6. Note that the variability of the blending times for a tank without coils is comparable to the test results obtained by Grenville and Tilton (Fig. 1), where the variation of the blending time with respect to the average value of the blending time is comparable. For the pilot scale tank with cooling coils installed, the variability, or scatter, of blending times increases.

Most test results are similar to Fig. 27 substitute, except the limiting case where the tank contents did not completely mix, which is shown in Figure 28. In this particular

test, some of the tracer quantity of base added to the tank was blended into solution while most of the basic solution remained on the tank bottom.

The recommended design conditions noted in Fig. 26 were related to pump design. In the author's opinions, the variability of the blending times between this value and a condition where blending was incomplete questioned the effectiveness of blender pump design. An engineering judgment recommended that  $UoD$  values below this limit should not be used for pump designs in a tank with coils installed. Note also, that Equation 1 seems to be less applicable as  $UoD$  decreases, and the blending time becomes less linear and the variability with respect to the average blending time increases.

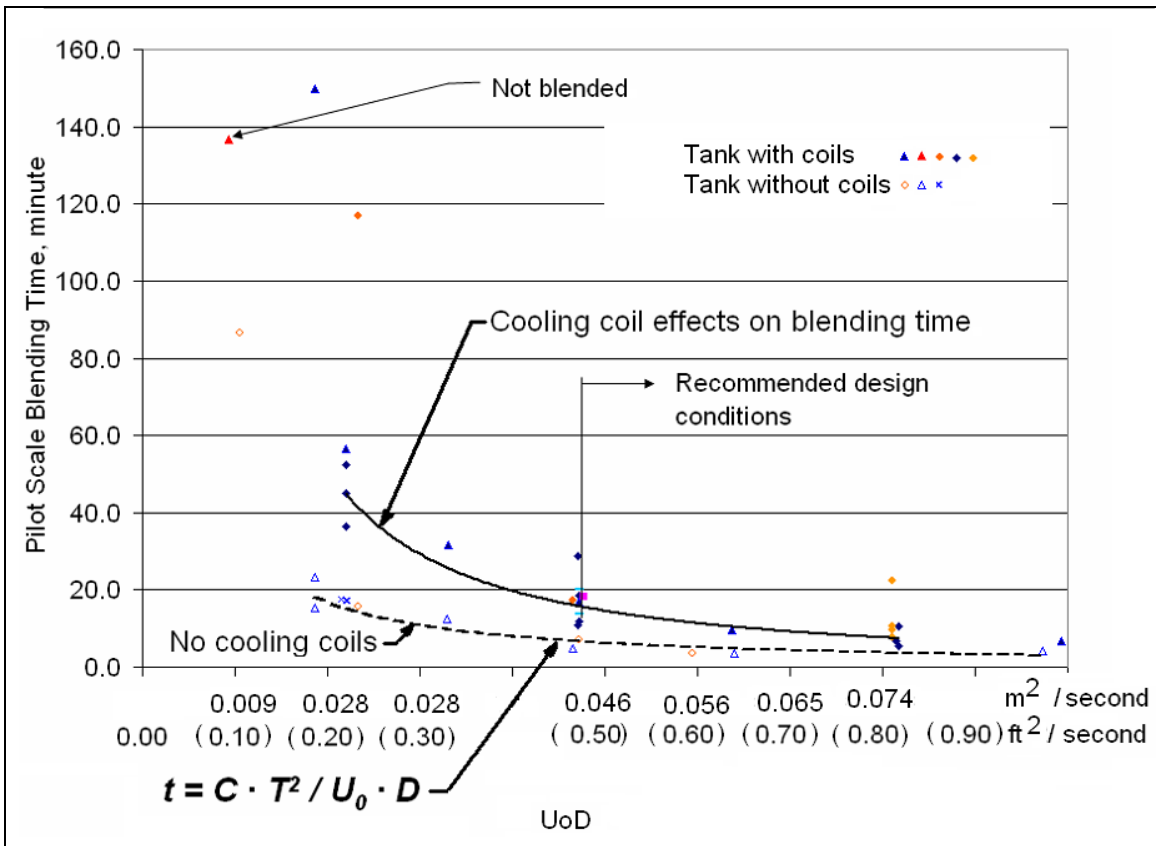


**Figure 26: Comparison of Phase 1 pilot scale test results for a tank with or without cooling coils**

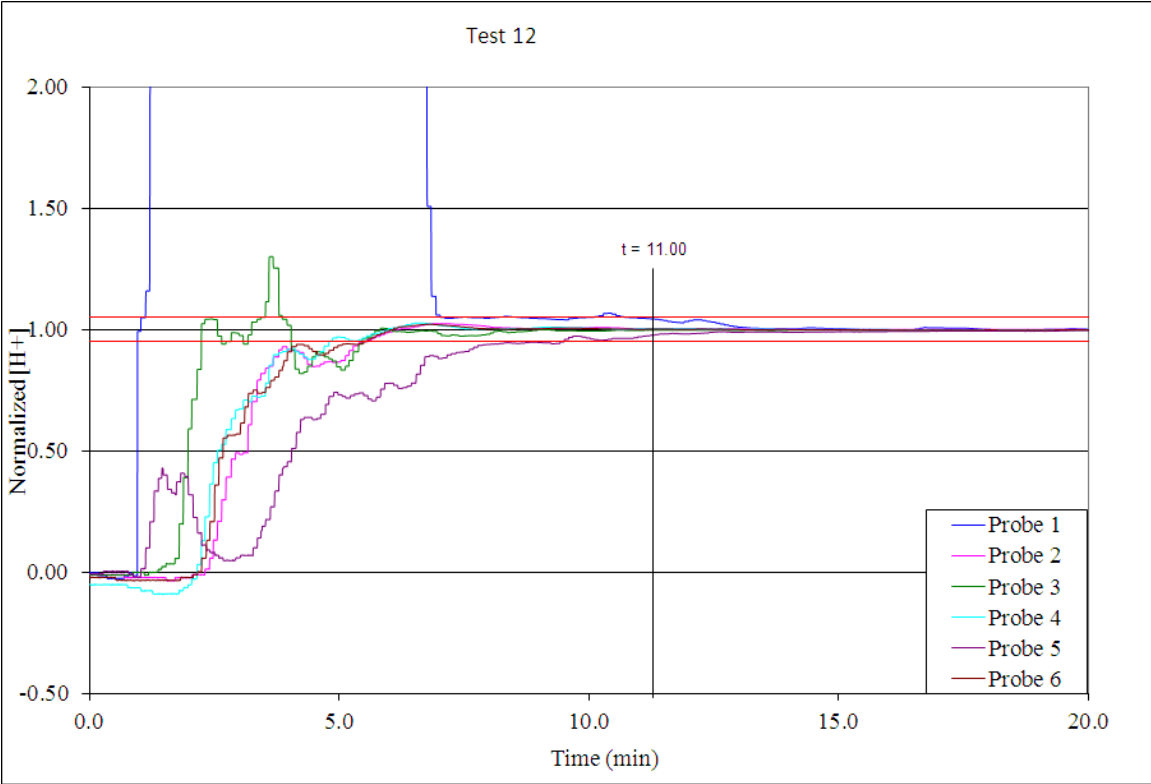


**Figure 27: Typical Blending Time Test Results**

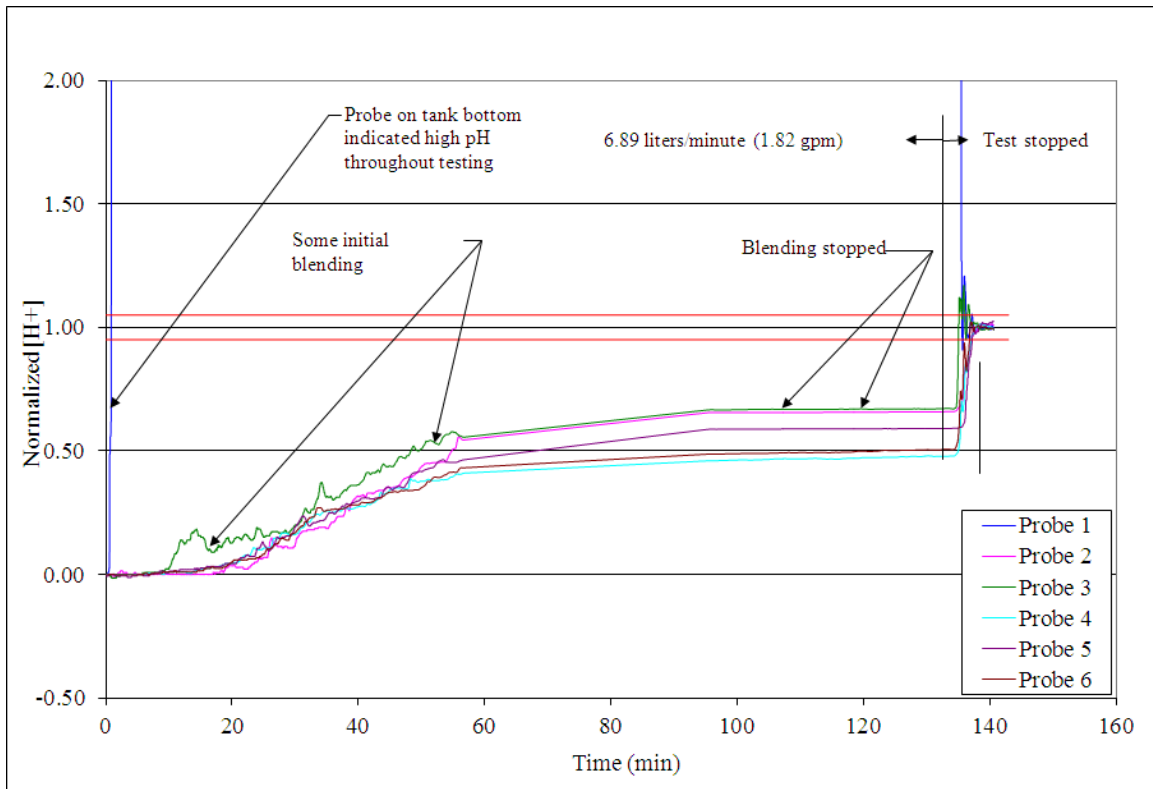


**Figure 28: Inadequate blending (Test 22)**

## PHASE 2 BLENDING RESULTS FOR TRACER SOLUTIONS

Phase 2 blending tests focused on final design requirements for the blending pump. Basically, Table 4 (Appendix A) summarizes the design parameters and test groupings, which were investigated and statistically analyzed in Phase 2 research. All of the pertinent test results from both Phase 1 and Phase 2 are displayed in Fig. 29, and the data in this figure were used to compare the effects of various parameters on blending times, where the average value of each set of tests is shown as a straight line for all of the probes in a related group of tests. Accordingly, the effects of any test parameter can be investigated, such as  $UoD$ , cooling coil installation, or type of fluid.

An important aspect of blending, chaotic behavior of the blending process became apparent during Phase 2 testing. A typical set of tests performed under similar conditions is shown in Fig. 30. Note the significant variation in blend times. This variation and the fact that the maximum blending time occurred at different probe locations throughout the tank is also evident in Tables 3 and 4, where the largest measured blending time for each test is noted in bold face type. Apparently, the complexity of adding coils or angled nozzles to the tank increased the variation of blending times with respect to an average blending time value. That is, the chaotic, random nature of blending increased, and the resultant blending time stochastic variability increased with system complexity.

Even the placements of pH probes to determine blending times were affected by the randomness of blending. A long standing practice for optimal probe placement was to do what seemed obvious. Add a dye to the tank, blend it until the dye disappeared, and then place the probe at the point which was last mixed to ensure that the maximum blending time was determined (Fox and Gex [19]). This research contradicted this practice, and showed that probe placement was irrelevant, since the last place to blend may occur anywhere in the tank. In fact, using a single probe to measure blending times may yield different blending times if the probe is installed at different locations in a tank.

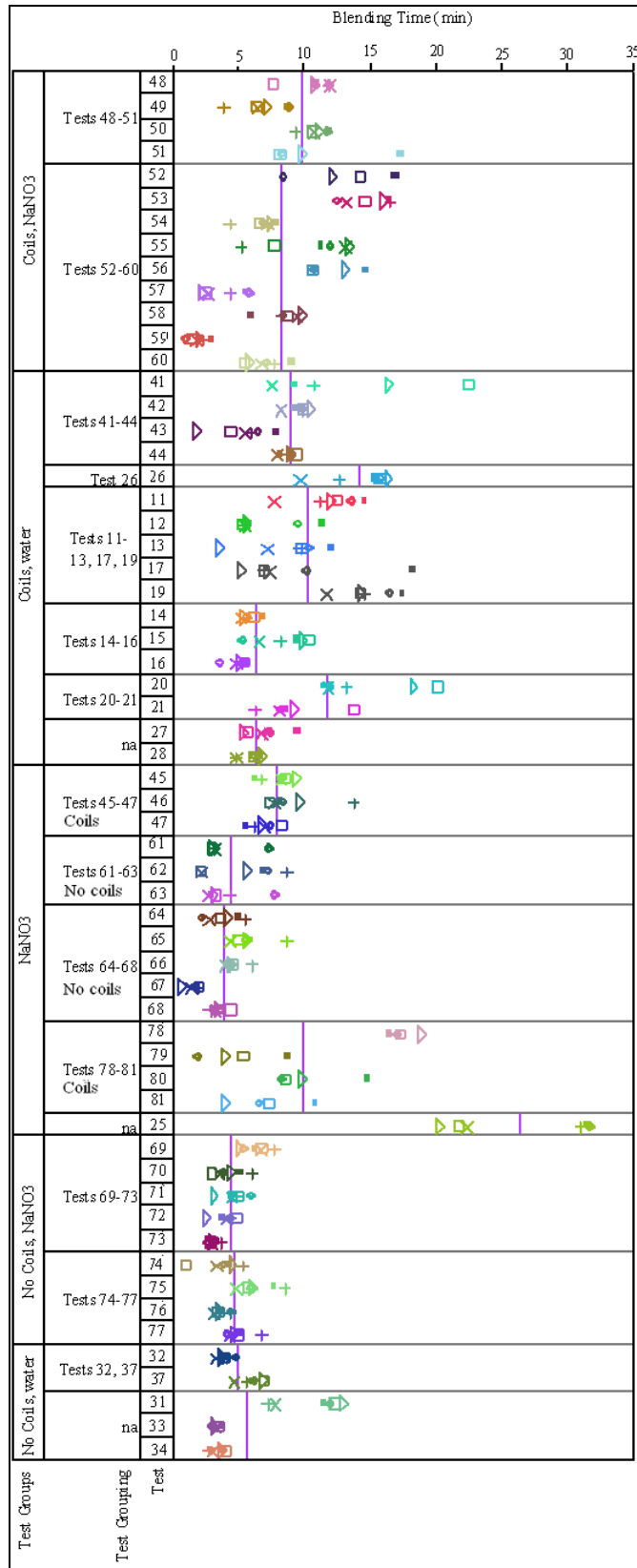
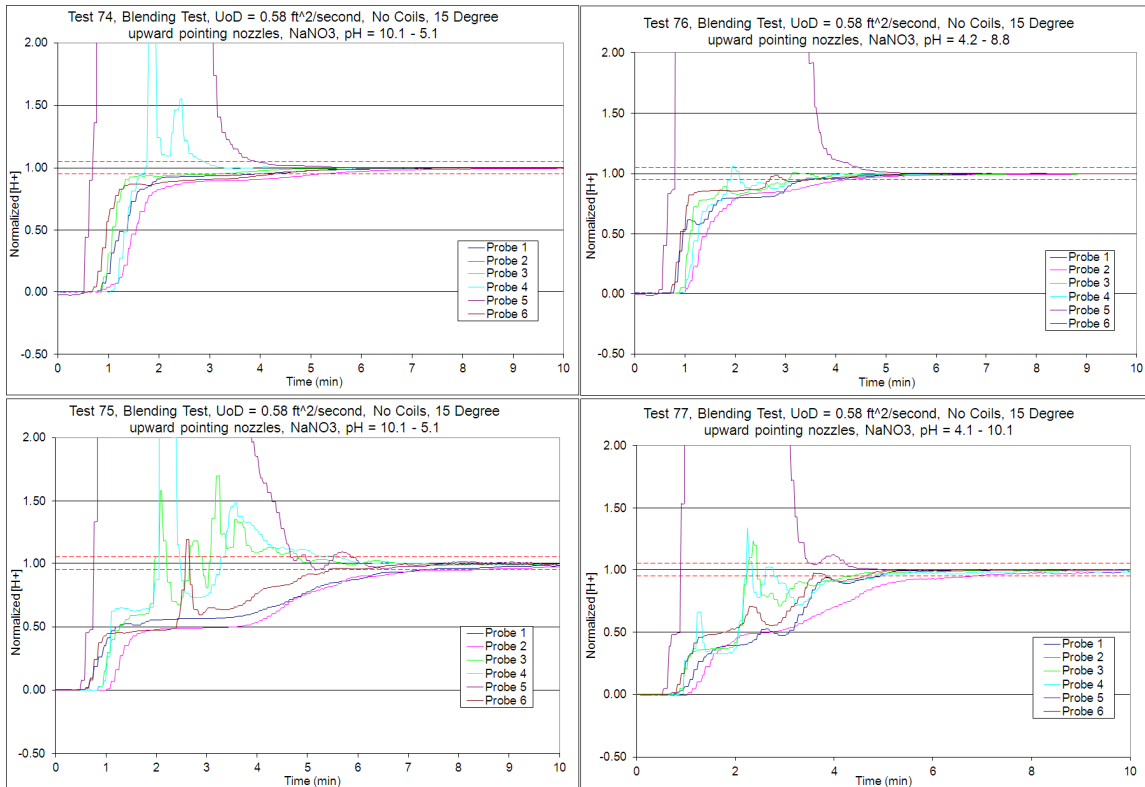


Figure 29: Summary of blending time results



**Figure 30: Typical set of blending time data**

## LIST OF BLENDING TEST RESULTS FOR TRACER ADDITIONS

The primary conclusions were that Equation 1 was adequate for simple blending processes like single or dual jet blending in tanks with few obstructions, but Equation 1 was inadequate to model complex blending processes when many obstructions were present in the tank. For these more complicated cases, CFD models were required along with experimental validation to establish correction factors to be applied to CFD results. To uphold this statement and establish correction factors, Phase 1 and 2 test data yielded numerous supporting test results:

1. The blending time predictions of Equation 1 for blending with a single nozzle were comparable for blending in the pilot scale tank without coils, even though the number of nozzles, nozzle locations, and tank geometry were different. That is, Equation 1 was adapted to provide an estimate of blending times for an SRS pilot scale tank without coils and dual opposing jets in the  $UoD$  range of interest. Above  $UoD > 0.031 \text{ m}^2/\text{second}$  ( $0.33 \text{ ft}^2/\text{second}$ ),

$$t = (C \cdot T^2) / (U_o \cdot D) = (3.72 \cdot T^2) / (U_o \cdot D) \quad (5)$$

2. Pilot scale blending times were significantly affected by cooling coil installation. Blending times in a tank with coils were twice the blending times for a tank without coils, within the recommended range of operation. Below the recommended range of operation for a tank with coils ( $UoD = 0.044 \text{ m}^2/\text{second}$  ( $0.47 \text{ ft}^2/\text{second}$ )), the basic fluid mechanics of blending are not understood, and blending times for a tank with coils were as much as seven times the blending time for a tank without coils at pilot scale. For similar  $UoD$  values, variability with respect to the average blending time was greater for a tank with coils than for a tank without coils.
3. For  $pH$  tests, pilot scale blending times were independent of initial and final concentrations of acid or base. For example, comparable blend times (11.0 and 11.9 minutes) were observed when the  $pH$  test range varied by either 5.86 or 1.52 (Tests 12 and 13 respectively). This observation validated the equivalence of many different tests, which had different starting and ending  $pH$  conditions.
4. Nozzle orientation with respect to the wall and changes in nozzle diameter had minor effects on blending times. A nozzle position parallel to the vertical tank

- wall was recommended for technical reasons outside the scope of this report (see [3]).
5. Nozzle diameter effects were not investigated outside the range of selected diameters (0.0035 meters (0.138 inches) and 0.0085 meters (0.334 inches). At smaller diameters, conclusions with respect to  $UoD$  and blending times may not be valid.
  6. A 95% blending time criterion was validated for use in test results, and obtaining a 99% blending time was questionable.
  7. Instrument uncertainties were negligible with respect to  $UoD$ . All variances in blend times were shown to be realistic expectations.
  8. Visual indications using blue dye additions to the tank instead of acid / base additions indicated much lower blending times than determined by using  $pH$  measurements. This observation was consistent with Grenville's observations on this topic [11 and 12].
  9. A negligible blending improvement was noted when nozzle designs were changed from a tee to the CW design (compare tests 61-63 to 64-68). This observation further demonstrated that  $UoD$  is the primary factor with respect to pump design, rather than specific pump nozzle design details.
  10. Changes in kinematic viscosity have a negligible effect on tracer blending when coils are installed (compare tests 78-81 to tests 48-51).
  11. From analysis of Fig. 26, the recommended minimum pilot scale, pump design requirements are  $UoD > 0.031$  meter<sup>2</sup>/second (0.33 feet<sup>2</sup>/sec) for a tank without coils, and  $UoD > 0.044$  meter<sup>2</sup>/second (0.47 feet<sup>2</sup>/sec) for a tank with coils.

Although blending can probably be performed at lower  $UoD$ 's than recommended, there was insufficient available data at lower  $UoD$  from test results and accompanying analysis.

12. Pilot scale blending times in a tank with coils varied by more than 100% for the same nozzle design and  $UoD$ . A review of test data concluded that blending times varied considerably for the same design conditions. For example, Tests 52 and 58 had similar test conditions, i.e.,  $pH$  conditions (7.3-10.4 and 7.4-10.8), operating temperatures (70° F and 71° F), fluids, procedures, and  $UoD$ . However, blending times varied by more than a factor of 2.3, when maximum blending times were 18.25 and 7.94 minutes, respectively. This example is characteristic of blending time results, where there was a large variation in blending times for apparently identical conditions.

## **CFD MODELS**

Numerous CFD models were performed for both pilot and full scale tanks for different pump designs (Lee and Armstrong [7]), where the blending pumps were installed at the mid-elevation, parallel to the tank wall as shown by typical results shown in Figs. 31 - 33. At pilot scale, CFD blending time predictions were within the range of experimental results, but variance of the predictions from experiment required investigation. Blending times were calculated using CFD, and also required evaluation.

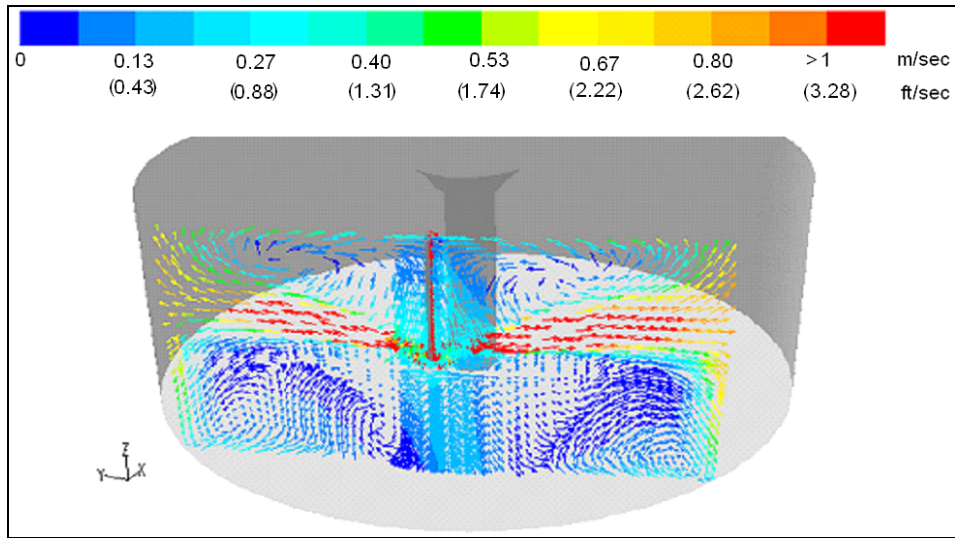


**Figure 31: Velocity in a pilot scale tank without coils at a vertical plane through upward pointing nozzles (Tests 74-77)**

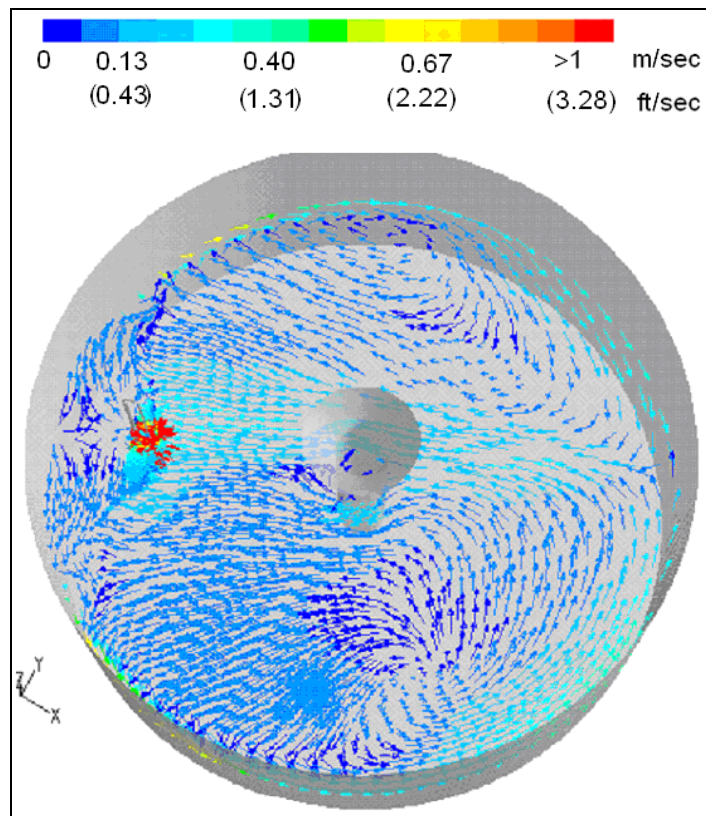


**Figure 32: Velocity in a pilot scale tank without coils at a horizontal plane through the horizontal centerline of the pump model (Tests 74-77)**

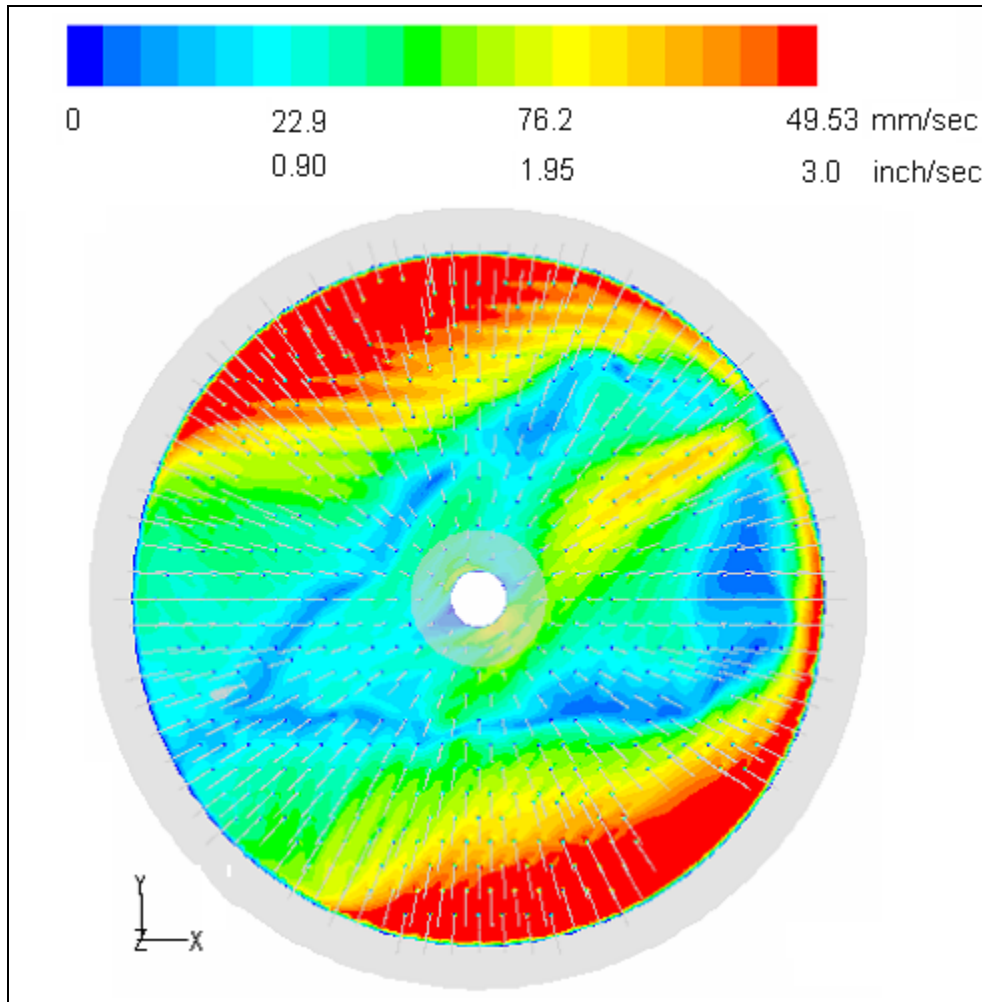


**Figure 33: Typical cross section of the pilot scale tank during blending (Tests 14 – 16, 25.4 mm (1 inch) above the tank floor)**

A three-dimensional computational fluid dynamics approach was used to calculate flow velocity distributions, and to estimate blending times for two miscible liquids. The results were benchmarked against both pilot scale test data and literature data. The commercial finite volume code, Fluent<sup>®</sup>, was used to create a full scale geometry file in a non-orthogonal mesh environment.

The domain was meshed by a hybrid meshing technique. The number of meshes for the domain with no cooling coils was  $1 \times 10^6$  nodes, as shown in Fig. 34. The number

of mesh nodes for the model with 560 cooling coils was  $4 \cdot 10^6$ . Figs. 35 and 36 show three-dimensional computational volume meshes and representative two-dimensional meshes near the pump and cooling coils for the tank model with cooling coils.

Similar to Patwardhan's work [13],  $\kappa$ - $\epsilon$  turbulence CFD models were used in this work to further investigate the effects of increasingly complex tank geometry and nozzle design on blending times in tanks blended with dual opposing jets, where the  $\kappa$ - $\epsilon$  models and mesh sizes were benchmarked in previous work (Lee, et al. [17 and 18]). For modeling calculations, the transient governing equations consisted of one mass balance, three momentum equations, two turbulence transport equations for kinetic energy ( $k$ ) and dissipation rate ( $\epsilon$ ), and one species transport equation. These equations were solved using an iterative technique until the species concentrations at all points in the tank met the 95% blending criteria, where the steady-state flow conditions for the tank were supplied as initial conditions. Fixed wall boundary conditions were assumed at the tank wall, coil surfaces, and floor of the tank. The free liquid surface was assumed to act as a flat, slip plane. The governing equations were solved over the entire tank domain for the cases of a tank with or without coils, where further details of those CFD calculations are available (Lee and Armstrong [7]).

Even so, the history of that work may be briefly summarized here. In earlier research, different turbulence models were investigated to assess measured velocities for a different pump design in an 85 foot diameter tank, and the  $\kappa$ - $\epsilon$  turbulence model provided the most accurate results for a tank without coils (Lee, et al. [17, 18]). Consequently, the  $\kappa$ - $\epsilon$  turbulence model was used in this research as well.

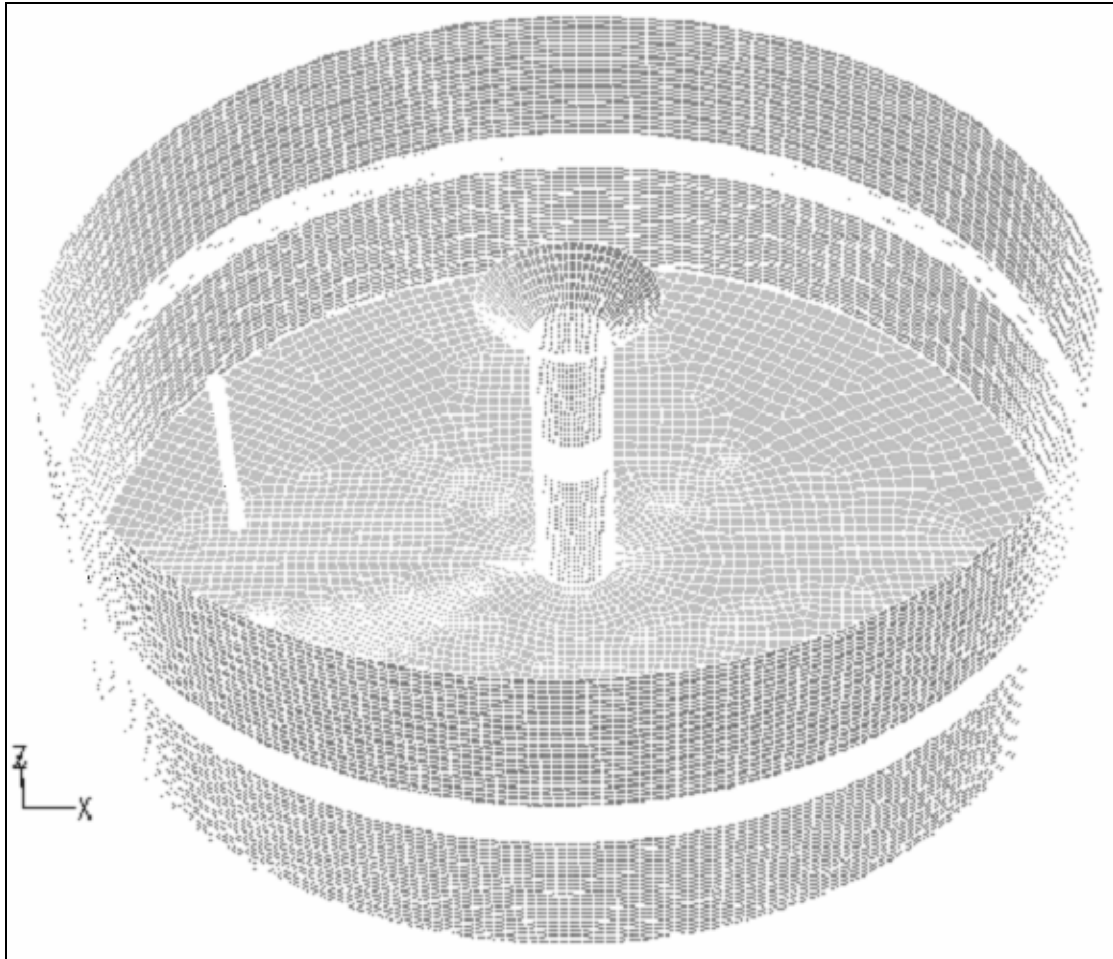


**Figure 34: Model geometry for a tank without coils**

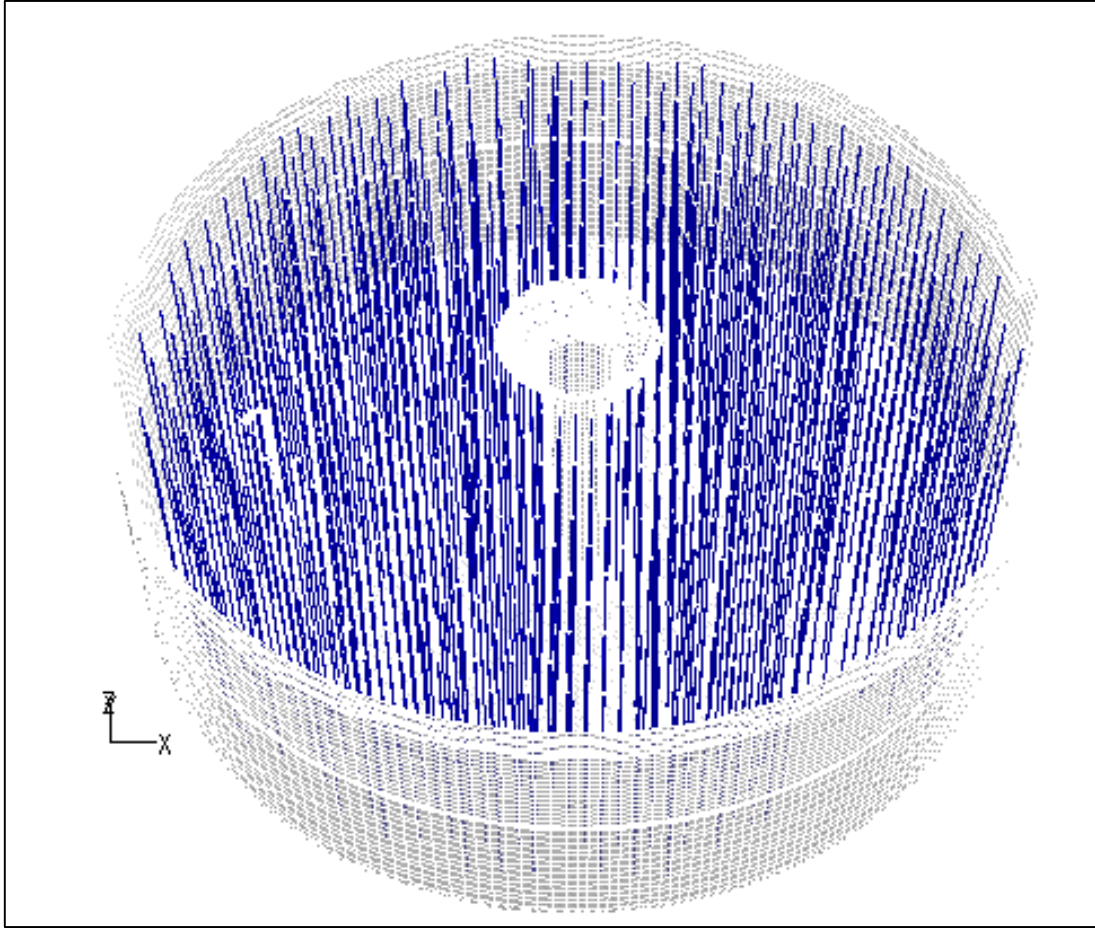


**Figure 35: Model geometry for a tank with coils**

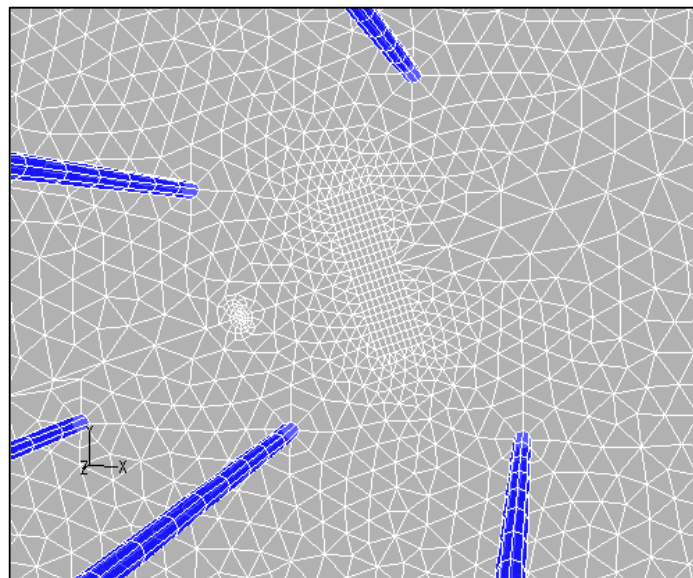


**Figure 36: Model geometry for a tank with coils near the pump nozzles**

## CFD RESULTS, EXPERIMENTS, AND STATISTICAL ANALYSIS

A comparison between CFD models and experimental results is presented in Figs. 37 and 38, where the CFD model results are in the range of experimental blending times. However, the large variance in experimental data for a tank required consideration. To do so, statistical analyses and engineering evaluations were performed to evaluate the variability of blending times, which were then used to establish a correction factor to be used with CFD models (Leishear, et al. [1, 6]).

Typical set of blending time data is shown in Figs. 20 and 27, and a summary of statistical test results is shown in Fig. 39, where additional data are available (Leishear, et al. [5, 6]). To estimate a scaling factor for blending, the statistical discussion provided in (Leishear, et al. [6]) needs to be related to experimental data. To do so, Fig. 39 provides two different variabilities for consideration, and one must be selected based on the nature of the tests performed. The typically larger variability (square symbol, UTL, upper tolerance limit for individual probes) provides a bound of values that would be predicted with 95% confidence if a single probe were installed in the tank to measure the blending time, and would only be used for the evaluation a blending time when a single probe is installed in a tank. The typically lower variability (diamond symbol, UTL on mean blend time) provides the bound at 95% confidence for predicted blending times for a set of tests. This latter variability is appropriately applied to test groups. In short, predicted CFD values are within 20 – 80% of the average experimental values (cross symbol, average of the blend times), but the predicted variation in blending times is even larger due to experimental variations in blending times.

To establish an experimental correction factor for CFD models, Fig. 39 bears further scrutiny. Test sets {20, 21} and {32, 37} are discounted, since insufficient data

points yielded questionable blending time predictions with very high resultant uncertainties. The rest of the data sets are pertinent to a correction factor.

Reviewing Fig. 39, the largest UTL data variance is shown to occur for test set {41-44}, which was the upper limiting case from available CFD modeling. For this data set, a preliminary pilot scale blending time correction factor,  $C_f$ , equals

$$C_f = (\text{UTL for mean blend time}) / (\text{CFD blend time}) = 28.33/10.73 = 2.64 \quad (6)$$

which may seem large, but the 2.64 correction factor provides a reasonable estimate at a 95% confidence level to correct CFD models at pilot scale. Although there was significant scatter in the blending times, the comparison of CFD predicted blending times to average experimental blending times was within 19% with 95% confidence (Tests {41-44}). The 2.64 value is recommended for the prediction of probable blending times using CFD models.

Similarly, for a tank without coils  $C_f = 12.82 / 7.4 = 1.74$  (Tests {74-77}). The variation between CFD predictions and the average blending time was within 67% with 95% confidence for the final pump design (Tests {74-77}).

These correction factors are based on experimental variation in pilot scale test data and differences between CFD and average blending times. The underlying physical explanation of this wide scatter in data was not fully investigated, since hundreds of additional experiments would have been required. Even so, experiments were carefully conducted to ensure that experimental results were consistent from test to test. In short, statistical analysis of experimental data was used to describe the complexities of chaotic

blending processes and obtain a correction factor to be applied to CFD models at pilot scale. Scale-up has been discussed in separate papers (Leishear, et al. [1, 2]), but further scale-up research is recommended.

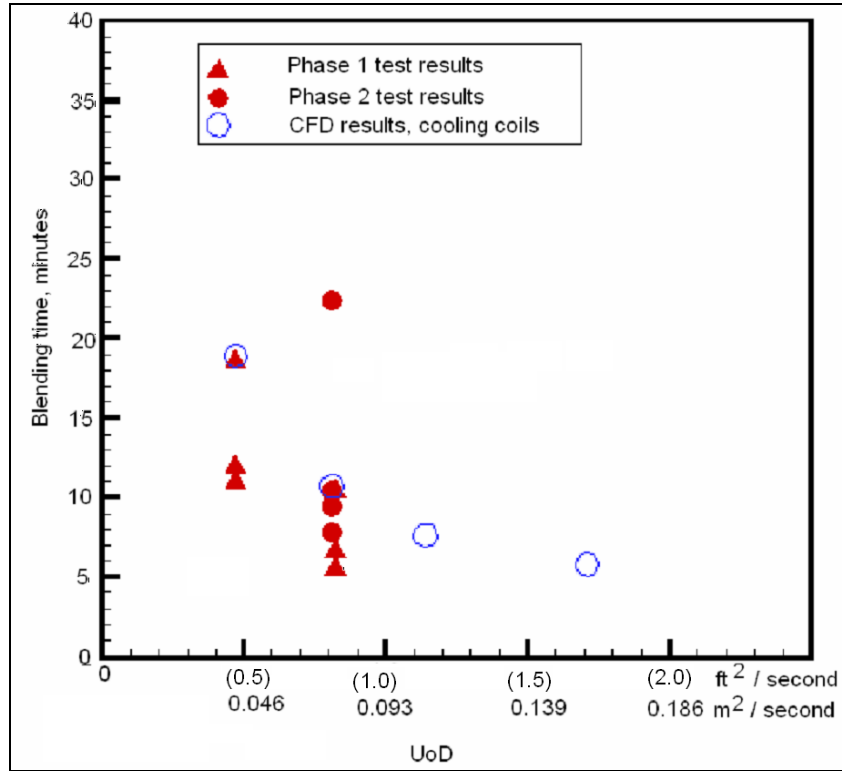


**Figure 37: Comparison of CFD results to experiments for a tank with coils installed**

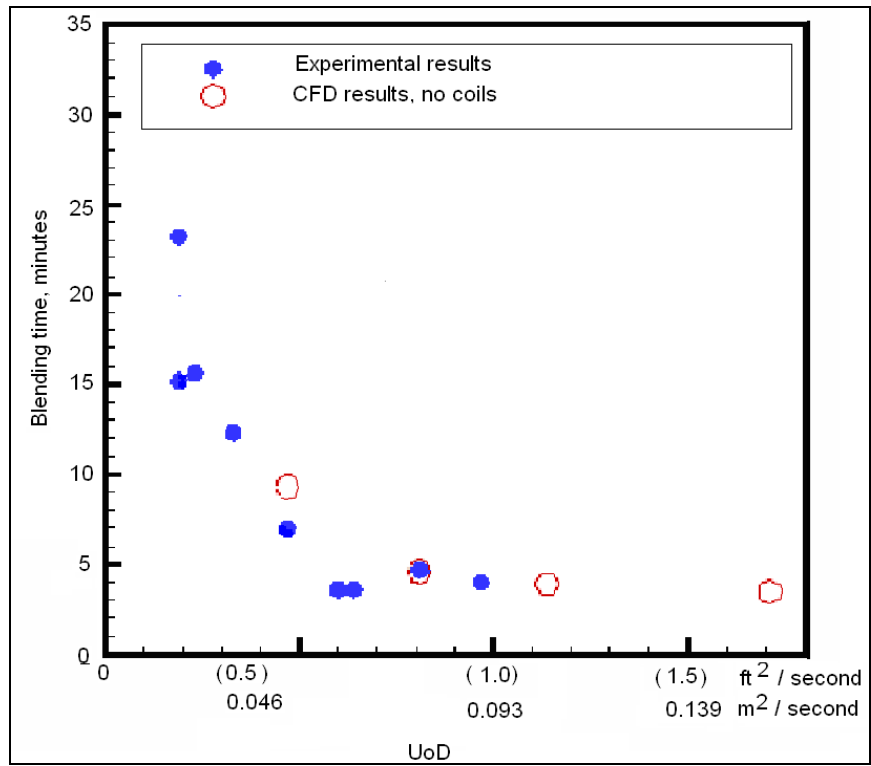


**Figure 38: Comparison of CFD results to experiments for a tank without coils installed**

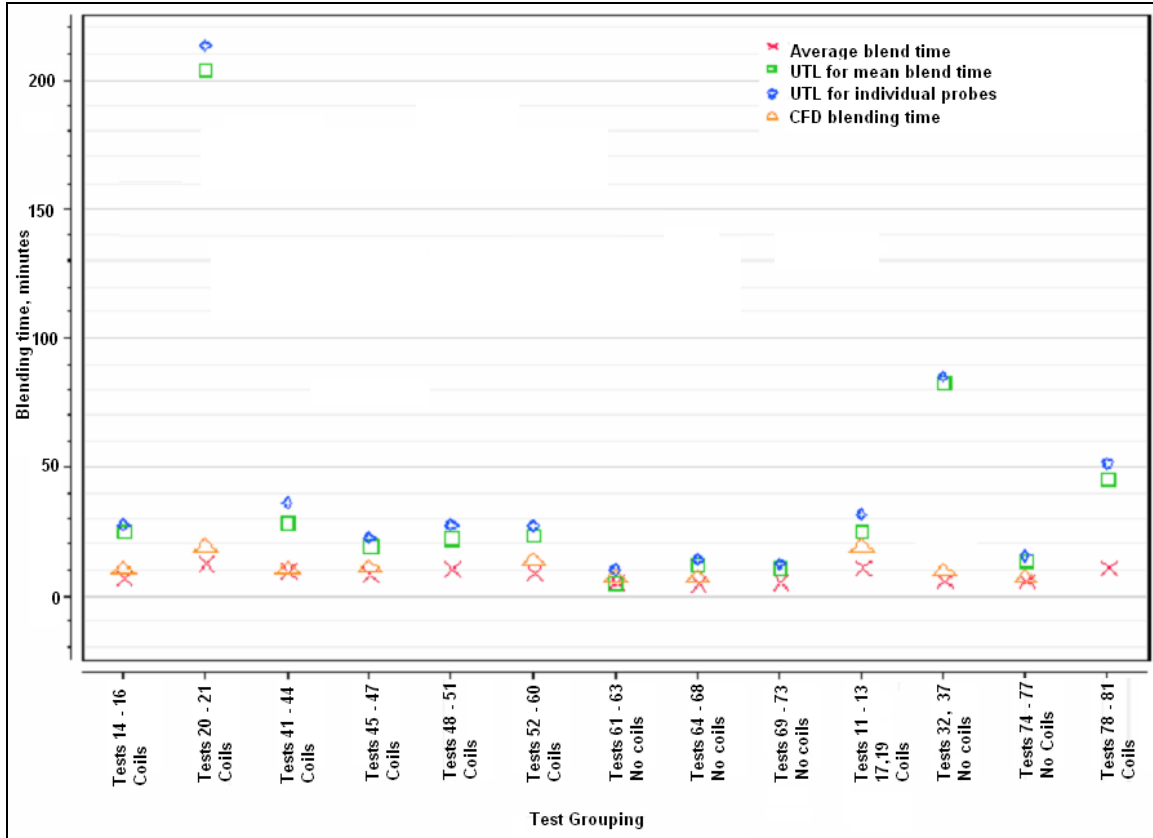


Figure 39: Data analysis (T. Edwards [6])

## TEST RESULTS FOR BLENDING DUE TO BULK TRANSFERS INTO THE PILOT SCALE TANK

The method of adding fluids to the tank affected blending. For these tanks, salt solutions were dropped into the tank from above the liquid level through a tube (Fig. 6). When heavier, or similar density, fluids were added to the tank, blending was completed solely by the mixing caused by the fluid addition as demonstrated by Figs. 40 and 41. However, when lighter fluids were added to heavier fluids, stratification significantly affected the blend time. For a much higher density salt solution of 2.26 centipoise and 1.32 grams/milliliter, the effects of stratification are shown in Figs. 42 and 43 in the form of stratification layer. An interface layer formed between the partially mixed water and

salt solution above the interface and the unmixed salt solution below the interface. Over time, this interface lowered as shown in Fig. 44. The blending time to lower the interface layer and completely blend the tank contents was 6.73 hours instead of an expected blending time of 8.4 minutes. The full scale blending time may scale up from several days to a week, or more. Even so, only a single test was performed for adding low to high density fluids and the effects of density and viscosity on blending were not evaluated for cases where the fluids had nearly equal densities. Additional research to investigate viscosity effects on blending is recommended, since the viscosities for these few tests were significantly different, where the viscosity equaled 2.68 centipoise for the  $\text{NaNO}_2$  solution vs. 1.0 centipoise for water.

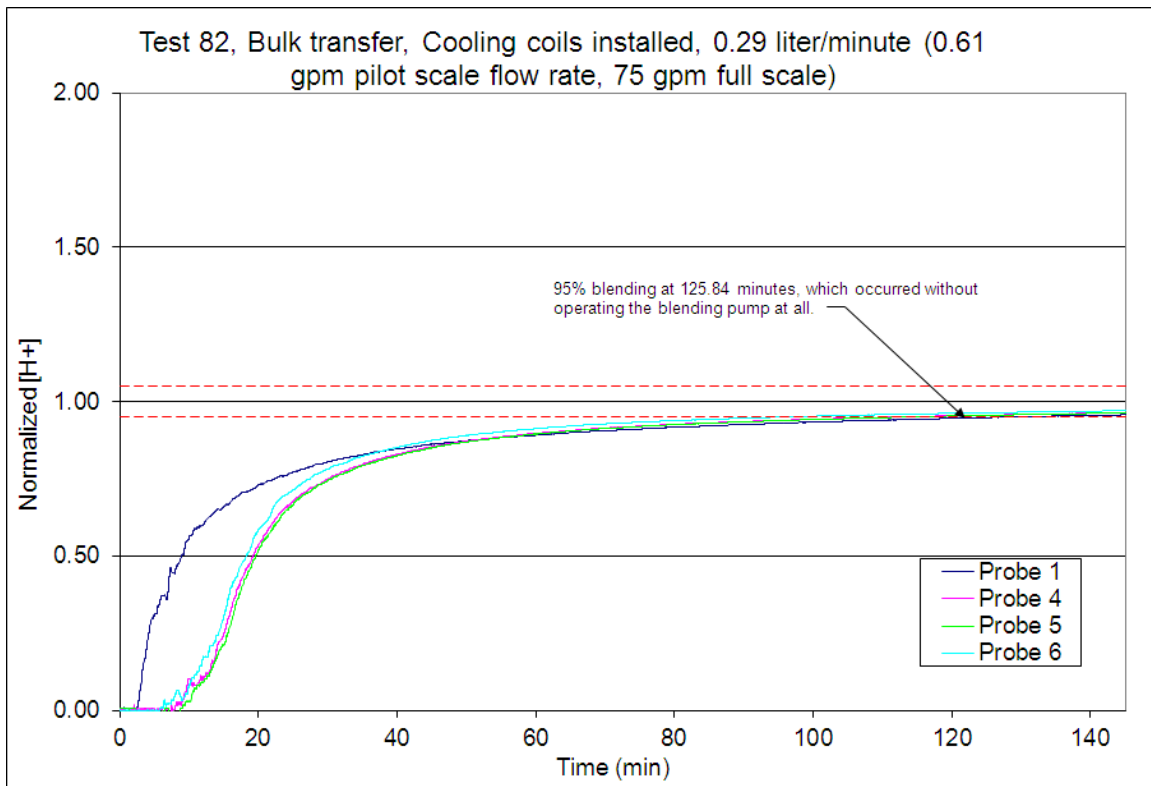
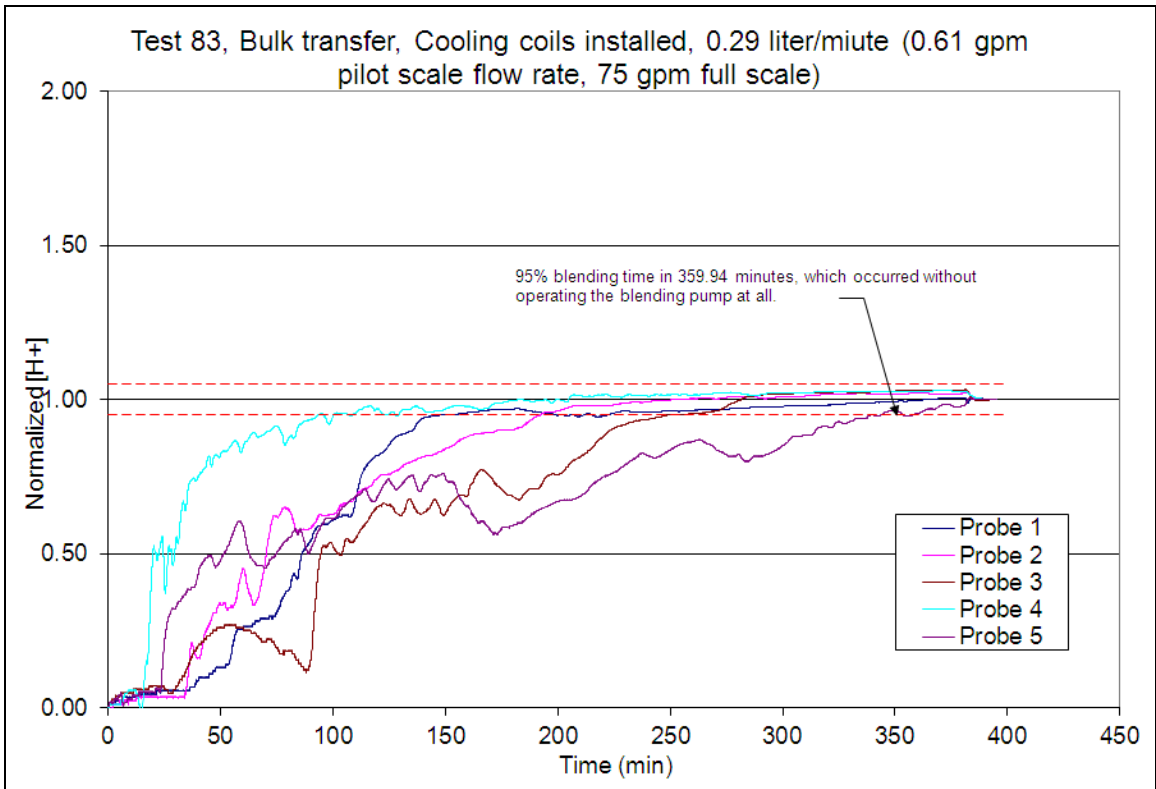
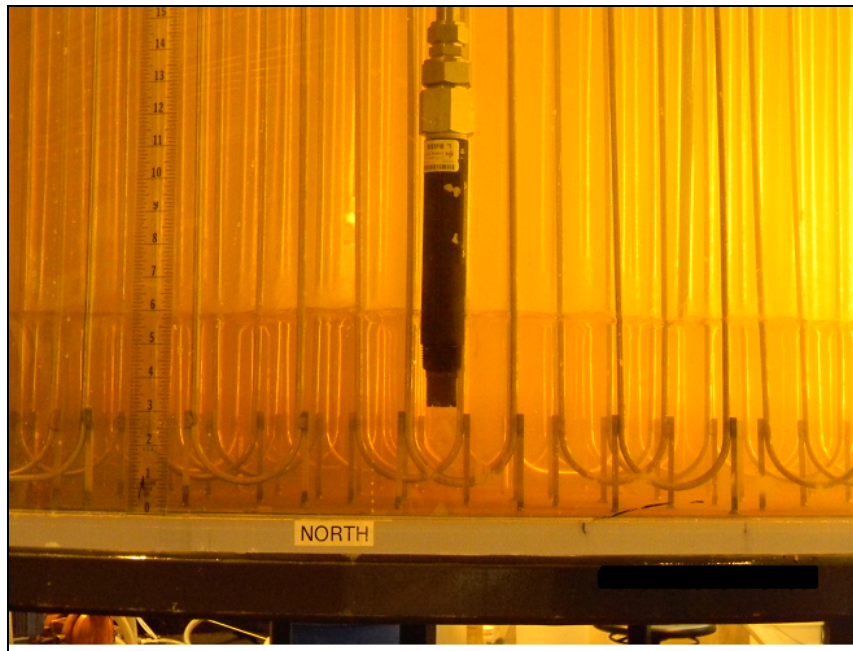


Figure 40: *pH* Measurements for transfer of  $\text{NaNO}_2$  to water



**Figure 41: *pH* Measurements for transfer of  $\text{NaNO}_2$  to  $\text{NaNO}_2$**



**Figure 42: Interface between salt solution layers, transfer of water into a salt solution (Test 84)**

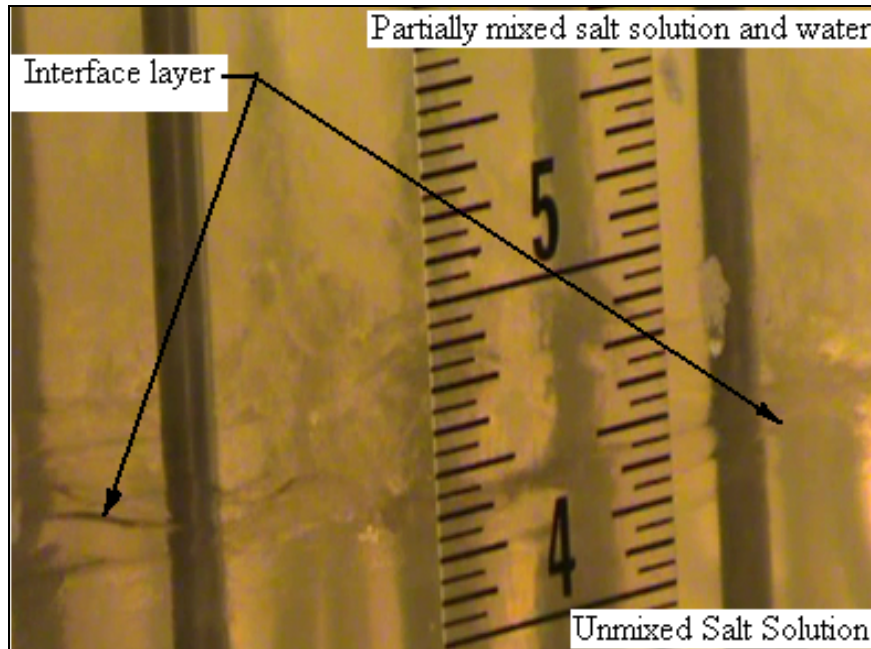


**Figure 43: Waves at interface layer, transfer of water into a salt solution (Test 84)**

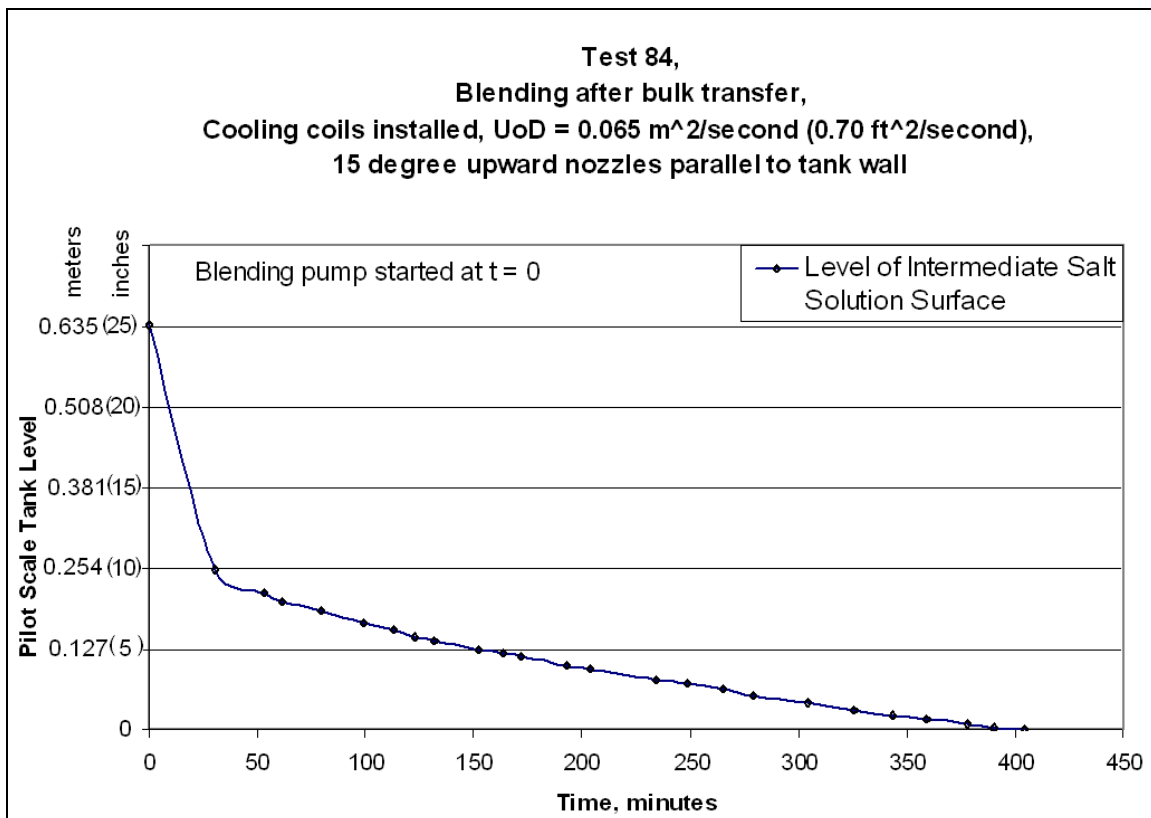


**Figure 44: Interface layer, level changes during blending of a stratified salt solution, transfer of water into salt solution**

## CONCLUSIONS

In short, equations can predict blending times for simple models, such as single or dual nozzle jets in tanks with few obstructions, but as the number of obstructions increase equations are inadequate to describe blending. For these more complex cases, CFD models with experimentally determined correction factors are required to determine blending times. Numerous experimental results are listed in this paper to support the primary conclusion that blending processes in tanks are chaotic and the random nature of blending times increase with system complexity, which affects CFD model predictions for blending times.

For simple geometry, such as a tank with a single jet, the blending process can be described by an equation that is accurate to within 24 % with 95% confidence for some cases. For the same geometry, CFD models had more than a 30% variation with respect to experiment.

For more complex models the variation in the blending time significantly increased, when dual opposing nozzles angled upward by 15 degrees were used in a 2.44 meter (8 foot) diameter pilot scale tank. In fact, CFD models for a tank without coils required a correction factor of 1.74 for use. When cooling coils were added, a correction factor of 2.64 was required to use pilot scale CFD models with 95 % confidence to obtain 95% blending. These observations of chaotic blending performance affect modeling, in that, errors in predicted blending times are possible when using CFD or empirical equations unless the experimentally observed variability is considered.

Research also observed stratification effects in some cases when blending different viscosity fluids that may significantly increase blending times. For example,

when water was added from above the tank to a highly viscous salt solution, the time required to blend the tank contents after addition was increased by a factor of about ten or more, but when base was added to water, blending was complete before the pump was started. All in all, much was learned about blending in tanks with internal obstructions, but some issues are yet to be resolved.

## **ACKNOWLEDGMENTS**

This research was performed for Savannah River Remediation, LLC, per direction of Keith Harp, Program Manager, Bill Van Pelt, Project Engineering Manager, Ken Parkinson, Lead Engineer, and Bob Ervin, Engineer, who each provided technical requirements and project leadership for this research.

In addition to the authors, a list of major contributors to this research included:

*SRNL Technician Staff:* Mike Armstrong, Vernon Bush, Andrew Foreman, Tim Forehand, Lowell Hicks, Chris Baxley, Victor Skeens, Steve Rikard, and Chris Rose.

*SRNL Managers and Staff:* Billy Giddings, Doug Sumpter, Sharon Marra, Steve Hensel, Patricia Lee, Frank Pennebaker, Michael Stowell, Leroy Williams, Tommy McCoy, and Jim Buchanan.

*SRNL Engineering Staff:* Mike Restivo, Michael Williams, Tommy Edwards, Mark Duignan, Chris Martino, John Pareizs, Erich Hansen, David Koopman, David Stefanko, David Best, David Missimer, Bruce Wiersma, and John Steimke.

## **NOMENCLATURE**

CFD            computational fluid dynamics

$C_f$	Blending time correction factor
$C'_i$	normalized concentration, grams/liter
$C_i$	measured variable concentration, grams/liter
$C_0$	initial concentration, grams/liter
CW	Curtiss Wright, Inc.
$C_\infty$	final equilibrium concentration, grams/liter
$D$	diameter, millimeters (inches)
$H$	tank height
$n$	percentage of blending
pH	- log of the Hydronium ion concentration
SRNL	Savannah River National Laboratory
SRS	Savannah River Site
SS	stainless steel
$t$	blending time, minutes
$t_n$	measured experimental blending time at a known percent of blending.
$T$	tank diameter, meters (feet)
TUR	turbidity
$U_0$	nozzle velocity, meter/second (feet/second)
$U_0D$	nozzle design parameter, meter <sup>2</sup> /second (ft <sup>2</sup> /second)

VEL	velocity
UTL	upper tolerance limit
Z	jet path length
$\varepsilon$	dissipation rate
$\kappa$	kinetic energy
$\sigma$	standard deviation

## REFERENCES

- [1] Leishear, R. A., Poirier, M. R., and Fowley, M. D., Lee, S. Y., Steeper, T. J., 2011, "Comparison of Experimental Results to CFD Models for Blending in a Tank Using Dual Opposing Nozzles", IMECE 2011-62042, International Mechanical Engineers Congress and Exposition, American Society of Mechanical Engineers, New York, New York, pp. 1-12.
- [2] Leishear, R. A., Fowley, M. D., Poirier, M. R., Lee, S. Y., and Steeper, T. J., 2011, "Blending Time and Velocity Variations During Blending in a Tank Using Dual Opposing Jets", IMECE2011-62116, International Mechanical Engineers Congress and Exposition, American Society of Mechanical Engineers, New York, New York, pp. 1-11.
- [3] Leishear, R. A., Fowley, M. D., Poirier, M. R., Lee, S. Y., Parkinson, K. S., and Steeper, T. J., 2011, "Incipient Sludge Mixing in Nuclear Waste Tanks During Salt Blending", Waste Management 2011 Conference, Phoenix, AZ, Paper No. 11086, pp. 1-14.
- [4] Leishear, R. A., Fowley, M. D., Poirier, M. R., Steeper, T. J., 2010, "Cooling Coil Effects On Blending in a Pilot Scale Tank", AIChE Annual Conference, New York, New York, pp. 1-30.
- [5] ] Leishear, R. A., Fowley, M. D., Poirier, M. R., "Leishear, R. A., Poirier, M. R., Fowley, M. D., "SDI Blend and Feed Blending Study, Tank 50H Scale Model for Blending Pump Design, Phase 1", SRNL-STI-2010-00054, pp. 1-100, Savannah River National Laboratory, Aiken, S. C.
- [6] Leishear, R. A., Poirier, M. R., and Fowley, M. D., "SDI Blend and Feed Blending Pump Design Phase 2", Savannah River National Laboratory, SRNL-STI-2010-00151, May 2011, Savannah River National Laboratory, Aiken, S. C, pp. 1-169.

- [7] Lee, S., Armstrong, B., "SDI, CFD Modeling Analysis", Savannah River National Laboratory, SRNL-STI-2011-00025, Savannah River National Laboratory, Aiken, S. C, pp. 1-67.
- [8] Lee, S. Y, Leishear, R. A., Poirier, M. R., 2012, "Tank 21 and Tank 24 Blend and Feed Study: Blending Times, Settling Times, and Transfers", Savannah River National Laboratory, SRNL-STI-2012-00306, Savannah River National Laboratory, Aiken, S. C, pp. 1-46.
- [9] Bai-Lin, H. 1984, "Chaos", World Scientific Publishing, Singapore, pp. 3-7.
- [10] R. A. Dimenna, S. Y. Lee, and D. A. Tamburello, 2011, "Advanced Mixing Models", SRNL-STI-2011-00026, Savannah River National Laboratory, S. C., pp. 1-66.
- [11] Grenville, R., Tilton, J., 1996, "A New Theory Improves the Correlation of Blend Time Data from Turbulent Jet Mixed Vessels", Trans. Inst. of Chem. Eng., Vol. 74, pp. 390-396.
- [12] Grenville, R., Tilton, J., 1997, "Turbulence or Flow as a Predictor of Blend Time in Turbulent Jet Mixed Vessels", Proceedings of the North European Conference on Mixing, pp. 67-74.
- [13] Patwardhan, A. W., 2002, "CFD Modeling of Jet Mixed Tanks", Chemical Engineering Science, **57**, pp. 1307-1318.
- [14] Rahimi and Parvareh, 2005, "Experimental and CFD Investigation on Mixing by a Jet in a Semi-Industrial Stirred Tank", Chemical Engineering Science, Pergamon Press, Miamisburg, Ohio, **115**, pp. 85-92.
- [15] Coleman, H. W., Steele, W. G., 2009, "Experimentation and Uncertainty Analysis for Engineers", John Wiley and Sons, New York, New York.
- [16] Paul, E. L., Atieno-Oberg, V. A., Kresta, S. M., Eds., 2004, "Handbook of Industrial Mixing", Brown, D. A. R., Jones, P. N., Middleton, J. C., "Experimental Methods", Hoboken, John Wiley and Sons, New Jersey, pp. 164 -174.
- [17] S. Y. Lee, R. A. Dimenna, R. A. Leishear, D. B. Stefanko, "Analysis of Turbulent Mixing Jets in a Large Scale Tank", Journal of Fluids Engineering, **130**, American Society of Mechanical Engineers, New York, New York, pp. 011104, 2008.
- [18] S. Y. Lee and R. A. Dimenna, 1995, "Validation Analysis for the Calculation of a Turbulent Free Jet in Water Using CFDS-FLOW3D and FLUENT (U)", WSRC-TR-95-0170, Savannah River National Laboratory, Aiken, S. C.
- [19] Fox, E. A., Gex, V. E., 1956 "Single-phase Blending of Liquids", AIChE Journal, **2**, pp. 539-544.

## APPENDIX A

### Table 3: Phase 1, Tabulated Blending Test Results

Phase 1														
Test	Test type, Nozzle design	Fluids	Coils	Nozzle position degrees	D mm (in)	Uo m/sec (ft/sec)	UoD m <sup>2</sup> /sec (ft <sup>2</sup> /sec)	Probe 1	Probe 2	Probe 3	Probe 4	Probe 5	Probe 6	
1	Blending, dye, Quad, Tee	Water, Dye	Y	0	8.48 (0.334)	2.41 (7.90)	0.02 (0.22)	N/A	N/A	N/A	N/A	N/A	N/A	
2	Blending, dye, Quad, Tee	Water, Dye	Y	90	8.48 (0.334)	2.43 (7.97)	0.02 (0.22)	N/A	N/A	N/A	N/A	N/A	N/A	
3	Blending, dye, Quad, Tee	Water, Dye	Y	45	8.48 (0.334)	2.35 (7.70)	0.019 (0.21)	N/A	N/A	N/A	N/A	N/A	N/A	
4	Diffusion, dye, Tee	Water, Dye	Y	N/A	N/A	0	0	N/A	N/A	N/A	N/A	N/A	N/A	
5	Diffusion, base, Tee	Water, Base	Y	N/A	N/A	0	0							
6	Diffusion, acid, Tee	Water, Acid	N	N/A	N/A	0	0							
7	Blending, Quad, Tee	Water, Base	Y	0	8.48 (0.334)	2.41 (7.89)	0.02 (0.22)							
8	Blending, Quad, Tee	Water, Acid	Y	0	8.48 (0.334)	2.41 (7.89)	0.02 (0.22)							
9	Blending, Quad, Tee	Water, Acid	Y	0	8.48 (0.334)	2.41 (7.90)	0.02 (0.22)							
10	Blending, Quad, Tee	Water Base	Y	0	8.48 (0.334)	5.16 (16.93)	0.044 (0.47)							
11	Blending, Quad, Tee	Water, Acid	Y	0	8.48 (0.334)	5.16 (16.94)	0.044 (0.47)	<b>14.41</b>	11.29	7.77	12.5	13.61	12.03	
12	Blending, Quad, Tee	Water, Acid	Y	0	8.48 (0.334)	5.16 (16.94)	0.044 (0.47)	<b>11.16</b>	5.55	5.5	5.4	9.53	5.59	
13	Blending, Quad, Tee	Water, Base	Y	0	8.48 (0.334)	5.16 (16.94)	0.044 (0.47)	<b>11.96</b>	9.79	7.22	9.72	10.45	3.63	
14	Blending, Quad, Tee	Water, Base	Y	0	8.48 (0.334)	8.93 (29.29)	0.076 (0.82)	<b>6.63</b>	5.71	5.2	6.25	5.71	5.32	
15	Blending, Quad, Tee	Water, Base	Y	0	8.48 (0.334)	8.95 (29.38)	0.076 (0.82)	9.23	8.25	6.53	<b>10.27</b>	5.33	9.83	
16	Blending, Quad, Tee	Water, Acid	Y	0	8.48 (0.334)	8.95 (29.38)	0.076 (0.82)	5.45	5.29	4.79	<b>5.52</b>	3.63	5.12	
17	Blending, Short Quad, Tee	Water, Base	Y	0	8.38 (0.330)	5.29 (17.35)	0.044(0.48)	<b>18.07</b>	6.98	7.39	6.97	10.22	5.21	
18	Blending, Standard, Tee	Water, Base	Y	0	3.40 (0.134)	6.38 (20.93)	0.022 (0.23)							
19	Blending, Standard, Tee	Water, Acid	Y	0	3.40 (0.134)	12.69 (41.64)	0.043 (0.46)	<b>17.28</b>	14.57	11.65	14.27	16.49	14.27	
20	Blending, Quad, Tee	Water, Acid, Dye	Y	90	8.48 (0.334)	5.16 (16.94)	0.044 (0.47)	11.35	13.31	11.86	<b>20.04</b>	12.03	18.22	
21	Blending, Quad, Tee	Water, Base	Y	90	8.48 (0.334)	5.16 (16.94)	0.044 (0.47)	8.37	6.36	8	<b>13.72</b>	8.22	9.28	
22	Not blended	Water, Acid	Y	45	8.48 (0.334)	1.02 (3.34)	0.009 (0.09)							
23	Blending, Quad, Tee Test stopped before blending completed	Water, Acid	Y	45	8.48 (0.334)	2.04 (6.70)	0.017 (0.19)							
24	Blending, Quad, Tee Test stopped before blending completed	Water, Base	Y	45	8.48 (0.334)	2.40 (7.89)	0.02 (0.22)							
25	Blending, Quad, Tee	Water, Acid	Y	45	8.48 (0.334)	3.63 (11.90)	0.031 (0.33)	31.38	31.05	22.33	21.64	<b>31.8</b>	20.31	
26	Blending, Quad, Tee	Water, Acid	Y	45	8.48 (0.334)	5.16 (16.94)	0.044 (0.47)	15.25	12.75	9.7	15.72	15.87	<b>16.34</b>	
27	Blending, Quad, Tee	Water, Base	Y	45	8.48 (0.334)	6.98 (22.89)	0.059 (0.64)	<b>9.38</b>	7.04	6.79	5.67	7.52	5.4	
28	Blending, Quad, Tee	Water, Base	Y	45	8.48 (0.334)	10.88 (35.71)	0.092 (0.99)	6.46	4.8	4.83	6.19	6.19	<b>6.8</b>	
29	Blending, Quad, Tee Test stopped before blending completed	Water, Acid	N	45	8.48 (0.334)	2.04 (6.70)	0.017 (0.19)							
30	Blending, Quad, Tee Test stopped before blending completed	Water, Base	N	45	8.48 (0.334)	2.04 (6.70)	0.017 (0.19)							
31	Blending, Quad, Tee	Water, Acid	N	45	8.48 (0.334)	3.61(11.85)	0.031 (0.33)	11.26	7.25	7.81	12.19	12.04	<b>12.95</b>	
32	Blending, Quad, Tee	Water, Base	N	45	8.48 (0.334)	5.10 (16.74)	0.044 (0.47)	3.61	4.23	3.36	3.9	<b>4.87</b>	3.73	
33	Blending, Quad, Tee	Water, Base	N	45	8.48 (0.334)	7.00 (22.98)	0.059 (0.64)	<b>3.61</b>	3.17	3.17	3.44	2.98	3.1	
34	Blending, Quad, Tee	Water, Acid	N	45	8.48 (0.334)	10.66 (34.99)	0.090 (0.97)	3.55	2.78	3.02	<b>4.07</b>	3.02	3.72	
35	Blending, Standard, Tee Test stopped before blending completed	Water, Acid	N	45	3.40 (0.134)	2.81 (9.22)	0.009 (0.105)							
36	Blending, Standard, Tee	Water, Base	N	45	3.40 (0.134)	6.38 (20.93)	0.022 (0.23)							
37	Blending, Standard, Tee	Water, Acid	N	45	3.40 (0.134)	12.89 (42.30)	0.044 (0.47)	5.99	5.72	4.65	<b>6.97</b>	6.24	6.9	
38	Blending, Standard, Tee	Water, Base	N	45	3.40 (0.134)	16.09 (52.81)	0.055 (0.60)							

**Table 4: Phase 2, Tabulated Blending Test Results**

Phase 2													
Test	Test type, Nozzle design	Initial fluid / Added fluid	Coils	Nozzle position degrees	D mm (in)	Uo m/sec (ft/sec)	UoD m <sup>2</sup> /sec (ft <sup>2</sup> /sec)	Probe 1	Probe 2	Probe 3	Probe 4	Probe 5	Probe 6
39	Blending, Design, Tee, Dye added to suction pipe	NaNO <sub>3</sub> , Dye	Y	0	5.31 (0.209)	14.20 (46.58)	0.075 (0.81)						
40	Blending, Design, Tee, Dye added to suction pipe	NaNO <sub>3</sub> , Dye	Y	0	5.31 (0.209)	14.20 (46.58)	0.075 (0.81)						
41	Blending, Design, Tee	Water	Y	0	5.31 (0.209)	14.20 (46.58)	0.075 (0.81)	9.17	10.72	7.54	<b>22.46</b>	N/A	16.46
42	Blending, Design, Tee	Water	Y	0	5.31 (0.209)	14.20 (46.57)	0.075 (0.81)	9.12	9.97	8.25	9.89	9.98	<b>10.47</b>
43	Blending, Design, Tee	Water	Y	0	5.31 (0.209)	14.20 (46.58)	0.075 (0.81)	<b>7.74</b>	6.03	5.47	4.41	6.52	1.80
44	Blending, Design, Tee	Water	Y	0	5.31 (0.209)	14.20 (46.58)	0.075 (0.81)	8.08	8.94	7.90	<b>9.31</b>	9.10	8.90
45	Blending, CW, 0 degree	NaNO <sub>3</sub> , 6.4 M	Y	0	5.21 (0.205)	14.44 (47.40)	0.075 (0.81)	6.15	6.78	8.31	8.54	8.40	<b>9.31</b>
46	Blending, CW, 0 degree	NaNO <sub>3</sub> , 6.4 M	Y	0	5.21 (0.205)	14.44 (47.39)	0.075 (0.81)	7.97	<b>13.87</b>	7.77	7.37	8.51	9.65
47	Blending, CW, 0 degree	NaNO <sub>3</sub> , 6.4 M	Y	0	5.21 (0.205)	14.44 (47.39)	0.075 (0.81)	5.41	6.18	6.95	<b>8.28</b>	7.55	6.81
48	Blending, CW, 15 degree	NaNO <sub>3</sub> , 6.4 M	Y	0	5.31 (0.209)	14.17 (46.48)	0.075 (0.81)	10.76	11.88	<b>11.95</b>	7.63	11.88	10.73
49	Blending, CW, 15 degree	NaNO <sub>3</sub> , 6.4 M	Y	0	5.31 (0.209)	14.17 (46.48)	0.075 (0.81)	8.54	3.96	6.49	6.35	<b>8.90</b>	7.23
50	Blending, CW, 15 degree	NaNO <sub>3</sub> , 6.4 M	Y	0	5.31 (0.209)	14.16 (46.47)	0.075 (0.81)	11.73	9.48	10.73	10.51	<b>11.76</b>	11.19
51	Blending, CW, 15 degree	NaNO <sub>3</sub> , 6.4 M	Y	0	5.31 (0.209)	14.16 (46.46)	0.075 (0.81)	17.20	N/A	N/A	8.14	8.40	9.77
52	Blending, CW, 15 degree	NaNO <sub>3</sub> , 6.4 M	Y	0	5.31 (0.209)	12.24 (40.16)	0.065 (0.70)	<b>16.71</b>	N/A	N/A	14.32	8.43	12.13
53	Blending, CW, 15 degree	NaNO <sub>3</sub> , 6.4 M	Y	0	5.31 (0.209)	12.24 (40.16)	0.065 (0.70)	16.29	<b>16.51</b>	13.24	14.58	12.53	15.97
54	Blending, CW, 15 degree	NaNO <sub>3</sub> , 6.4 M	Y	0	5.31 (0.209)	12.24 (40.17)	0.065 (0.70)	7.72	4.36	7.15	6.55	6.95	7.38
55	Blending, CW, 15 degree	NaNO <sub>3</sub> , 6.4 M	Y	0	5.31 (0.209)	12.24 (40.17)	0.065 (0.70)	11.11	5.24	13.13	7.69	11.99	<b>13.41</b>
56	Blending, CW, 15 degree	NaNO <sub>3</sub> , 6.4 M	Y	0	5.31 (0.209)	12.24 (40.16)	0.065 (0.70)	<b>14.52</b>	N/A	N/A	10.65	10.73	13.07
57	Blending, CW, 15 degree	NaNO <sub>3</sub> , 6.4 M	Y	0	5.31 (0.209)	12.24 (40.16)	0.065 (0.70)	5.32	4.53	2.68	2.51	<b>5.92</b>	2.28
58	Blending, CW, 15 degree	NaNO <sub>3</sub> , 6.4 M	Y	0	5.31 (0.209)	12.24 (40.17)	0.065 (0.70)	5.81	8.34	9.48	8.71	8.48	<b>9.79</b>
59	Blending, CW, 15 degree	NaNO <sub>3</sub> , 6.4 M	Y	0	5.31 (0.209)	12.24 (40.16)	0.065 (0.70)	<b>2.82</b>	2.48	1.79	1.45	1.11	2.08
60	Blending, CW, 15 degree	NaNO <sub>3</sub> , 6.4 M	Y	0	5.31 (0.209)	12.24 (40.16)	0.065 (0.70)	<b>8.94</b>	7.69	6.75	5.44	7.18	5.81
61	Blending, Design, Tee	NaNO <sub>3</sub> , 6.4 M	N	0	5.31 (0.209)	12.24 (40.16)	0.075 (0.81)	3.19	3.19	3.25	2.99	<b>7.43</b>	3.02
62	Blending, Design, Tee	NaNO <sub>3</sub> , 6.4 M	N	0	5.31 (0.209)	14.17 (46.48)	0.075 (0.81)	6.81	<b>8.80</b>	2.16	2.14	7.29	5.67
63	Blending, Design, Tee	NaNO <sub>3</sub> , 6.4 M	N	0	5.31 (0.209)	14.16 (46.47)	0.075 (0.81)	2.79	4.41	2.68	3.22	<b>7.83</b>	3.07
64	Blending, CW, 0 degree	NaNO <sub>3</sub> , 6.4 M	N	0	5.21 (0.205)	14.44 (47.38)	0.075 (0.81)	4.78	<b>5.61</b>	2.79	3.62	2.25	4.21
65	Blending, CW, 0 degree	NaNO <sub>3</sub> , 6.4 M	N	0	5.21 (0.205)	14.44 (47.38)	0.075 (0.81)	5.64	<b>8.80</b>	4.44	4.95	5.58	5.64
66	Blending, CW, 0 degree	NaNO <sub>3</sub> , 6.4 M	N	0	5.21 (0.205)	14.45 (47.40)	0.075 (0.81)	4.13	<b>6.15</b>	4.01	4.67	4.41	4.38
67	Blending, CW, 0 degree	NaNO <sub>3</sub> , 6.4 M	N	0	5.21 (0.205)	14.45 (47.40)	0.075 (0.81)	1.65	1.91	1.42	<b>2.02</b>	1.68	0.74
68	Blending, CW, 0 degree	NaNO <sub>3</sub> , 6.4 M	N	0	5.21 (0.205)	14.44 (47.38)	0.075 (0.81)	2.99	2.93	3.27	<b>4.41</b>	3.79	3.39
69	Blending, CW, 15 degree	NaNO <sub>3</sub> , 6.4 M	N	0	5.31 (0.209)	14.17 (46.48)	0.075 (0.81)	6.12	<b>7.83</b>	6.63	6.81	5.44	5.01
70	Blending, CW, 15 degree	NaNO <sub>3</sub> , 6.4 M	N	0	5.31 (0.209)	14.17 (46.48)	0.075 (0.81)	4.90	<b>6.15</b>	3.56	3.05	3.87	4.44
71	Blending, CW, 15 degree	NaNO <sub>3</sub> , 6.4 M	N	0	5.31 (0.209)	14.17 (46.499)	0.075 (0.81)	4.19	4.98	4.53	4.93	<b>5.98</b>	3.16
72	Blending, CW, 15 degree	NaNO <sub>3</sub> , 6.4 M	N	0	5.31 (0.209)	14.17 (46.48)	0.075 (0.81)	3.64	4.50	4.04	<b>4.84</b>	4.41	2.53
73	Blending, CW, 15 degree	NaNO <sub>3</sub> , 6.4 M	N	0	5.31 (0.209)	14.17 (46.48)	0.075 (0.81)	3.19	<b>3.76</b>	2.99	2.93	2.79	2.96
74	Blending, CW, 15 degree	NaNO <sub>3</sub> , 6.4 M	N	0	5.31 (0.209)	10.15 (33.29)	0.054 (0.58)	4.07	<b>5.38</b>	3.36	1.04	3.99	4.47
75	Blending, CW, 15 degree	NaNO <sub>3</sub> , 6.4 M	N	0	5.31 (0.209)	10.15 (33.29)	0.054 (0.58)	7.52	<b>8.60</b>	4.87	5.69	6.01	6.15
76	Blending, CW, 15 degree	NaNO <sub>3</sub> , 6.4 M	N	0	5.31 (0.209)	10.15 (33.29)	0.054 (0.58)	3.45	4.36	3.10	3.42	<b>4.53</b>	3.56
77	Blending, CW, 15 degree	NaNO <sub>3</sub> , 6.4 M	N	0	5.31 (0.209)	10.15 (33.29)	0.054 (0.58)	4.95	<b>6.92</b>	4.44	5.01	4.24	4.70
78	Blending, CW, 15 degree	NaNO <sub>3</sub> , 3.2 M	Y	0	5.31 (0.209)	14.17 (46.48)	0.075 (0.81)	16.23	N/A	N/A	17.31	17.03	18.91
79	Blending, CW, 15 degree	NaNO <sub>3</sub> , 3.2 M	Y	0	5.31 (0.209)	14.17 (46.49)	0.075 (0.81)	<b>8.57</b>	N/A	N/A	5.38	1.96	4.02
80	Blending, CW, 15 degree	NaNO <sub>3</sub> , 3.2 M	Y	0	5.31 (0.209)	14.17 (46.48)	0.075 (0.81)	<b>14.64</b>	N/A	N/A	8.63	8.37	9.74
81	Blending, CW, 15 degree	NaNO <sub>3</sub> , 3.2 M	Y	0	5.31 (0.209)	14.17 (46.48)	0.075 (0.81)	<b>10.62</b>	N/A	N/A	7.32	6.63	3.93
82	Bulk transfer, salt to water, CW, 15 degree	NaNO <sub>3</sub> , 6.4 M / water	Y	0	N/A	N/A	N/A						
83	Bulk transfer, salt to salt, CW, 15 degree	NaNO <sub>3</sub> , 6.4 M / NaNO <sub>3</sub> , 6.4 M water	Y	0	N/A	N/A	N/A						
84	Bulk transfer, water to salt, CW, 15 degree	water / NaNO <sub>3</sub> , 6.4 M	Y	0	5.31 (0.209)	12.24 (40.16)	0.065 (0.70)						
85	Bulk transfer, water to water, CW, 15 degree	water / water	Y	0	N/A	N/A	N/A						